Formation of a unusually short hydrogen bond in photoactive yellow protein

*Keisuke Saito [1, 2] and Hiroshi Ishikita [1, 2]**

1) 202 Building E, Career-Path Promotion Unit for Young Life Scientists, Graduate School of Medicine, Kyoto University, Yoshida-Konoe-cho, Sakyo-ku, Kyoto 606-8501, Japan

2) Japan Science and Technology Agency (JST), PRESTO, 4-1-8 Honcho Kawaguchi, Saitama 332-0012, Japan

Running Title: Short H bonds in photoactive yellow protein

CORRESPONDING AUTHOR: Ishikita, 202 Building E, Career-Path Promotion Unit for Young Life Scientists, Graduate School of Medicine, Kyoto University, Yoshida-Konoe-cho, Sakyo-ku, Kyoto 606-8501, Japan, Tel. +81-75-753-9286, Fax. +81-75-753-9286, **E-mail:** hiro@cp.kyoto-u.ac.jp

Abbreviations:

δ_H, ^{1}H NMR chemical shift (δ_H);

FTIR spectroscopy, Fourier transform infrared spectroscopy;

LBHB, low-barrier hydrogen bond;

*p*CA, *p*-coumaric acid;

PYP, Photoactive yellow protein;

QM/MM, quantum mechanical/molecular mechanical;

ABSTRACT

The photoactive chromophore of photoactive yellow protein (PYP) is *p*-coumaric acid (*p*CA). In the ground state, the *p*CA chromophore exists as a phenolate anion, which is H-bonded by protonated Glu46 (O_{Glu46}–O_{pCA}= ~2.6 Å) and protonated Tyr42. On the other hand, the O_{Glu46}–O_{pCA} H-bond was unusually short (O_{Glu46}–O_{pCA}=2.47 Å) in the intermediate pR_{CW} state observed in time-resolved Laue diffraction studies. To understand how the existence of the unusually short H-bond is energetically possible, we analyzed the H-bond energetics adopting a quantum mechanical/molecular mechanical (QM/MM) approach based on the atomic coordinates of the PYP crystal structures. In QM/MM calculations, the O_{Glu46}–O_{pCA} bond is 2.60 Å in the ground state, where Tyr42 donates a H-bond to *p*CA. In contrast, when the hydroxyl group of Tyr42 is flipped away from *p*CA, the H-bond was significantly shortened to 2.49 Å in the ground state. The same H-bond pattern reproduced the unusually short H-bond in the pR_{CW} structure (O_{Glu46}–O_{pCA}=2.49 Å). Intriguingly, the potential-energy profile resembles that of a single-well H-bond, suggesting that the pK_a values of the donor (Glu46) and acceptor (*p*CA) moieties are nearly equal. The present results indicate that the "equal pK_a" requirement for formation of single-well or low-barrier H-bond (LBHB) is satisfied only when Tyr42 does not donate a H-bond to *p*CA, and argue against the possibility that the O_{Glu46}–O_{pCA} bond is an LBHB in the ground state, where Tyr42 donates a H-bond to *p*CA.

Keywords: low-barrier hydrogen bond, proton transfer, photoactive yellow protein, Laue diffraction crystallography, ^{1}H-NMR

1. INTRODUCTION

Photoactive yellow protein (PYP) serves as a bacterial photoreceptor, in particular, as a sensor for negative phototaxis to blue light [1]. The photoactive chromophore of PYP is *p*-coumaric acid (*p*CA), which is covalently attached to Cys69 [2]. In the PYP ground state, the *p*CA chromophore exists as a phenolate anion [3-5]. The PYP crystal structure revealed that *p*CA is H-bonded by protonated Tyr42 and protonated Glu46 (Figure 1). Tyr42 is further H-bonded by Thr50. Structural analysis suggested that Glu46 is protonated and *p*CA is ionized in the PYP ground state, pG [6, 7]. H atom positions of PYP were assigned in neutron diffraction analysis [8]. According to neutron diffraction analysis, in the case of the Glu46–*p*CA pair, an H atom was at a distance of 1.21 Å from Glu46 and 1.37 Å from *p*CA, almost at the midpoint of the O_{Glu46}–O_{pCA} bond (2.57 Å) (Figure 1). From this unusual H atom position, the H bond between Glu46 and *p*CA was interpreted as a low-barrier H bond [8].

An low-barrier hydrogen bond (LBHB) is a non-standard H bond, which was originally proposed to possess covalent bond-like characteristics, thus significantly stabilizing the transition state and facilitating enzymatic reactions [9, 10]. In original reports by Frey et al. [10] and Cleland and Kreevoy [9], it was stated that an LBHB (including a single-well H-bond) can form when the pK_a difference between donor and acceptor moieties is nearly zero (Figure 1). If this is the case, the identification of an LBHB with a single minimum potential can be valid only if the minimum is at the center of the O_{Glu46}–O_{pCA} bond (i.e., the pK_a values of the two moieties are nearly equal) as suggested by Schutz and Warshel [11]. It has been suggested that a stronger H bond results in a more downfield ^{1}H NMR chemical shift. According to the classification of H bonds by Jeffrey [12] and Frey [13], "single-well H bonds" are very short, typically with O–O distances of 2.4 to 2.5 Å, and display ^{1}H NMR chemical shifts (δ_H) of 20 to 22 ppm [13]. "LBHBs" are longer, 2.5 to 2.6 Å, with a δ_H of 17 to 19 ppm [13]. "Weak H-bonds" are even longer, with a δ_H of 10 to 12 ppm [13].

Upon exposure to blue light, PYP undergoes the following photocycle; pG (ground state) → P* –(*trans-cis* isomerization)→ I_0 → $I_0^{\ddagger}$ → pR –(proton transfer and large conformational change)→ pB → pG [14-16]. The pR to pB transition has been suggested to involve protonation of *p*CA (i.e., proton

transfer) and a large structural change of the protein [14, 15]. Although time-resolved Laue diffraction studies proposed structural models of the intermediates [17], the relevance of the proposed pB structure (PDB: 1TS0) as an intermediate of the photocycle is a matter of debate. In Laue diffraction studies, the pB intermediate has a H-bond between Arg52 and *p*CA [17], whereas solution structures of the pB state argue a high degree of disorder in residues 42-56 [18] (discussed in Ref. [19]).

On the other hand, time-resolved Laue diffraction studies identified the pR_{CW} intermediate [17]. The pR_{CW} intermediate structure [17] was proposed to correspond to the pR species [14-16] observed in spectroscopic studies. The pR state decays to the pB state as a result of PT from Glu46 to *p*CA with the rate coefficient of 250 μs [14, 15], which is consistent with that of 333 μs for the pR_{CW} decay [17]. To our best knowledge solution structures of the pR state have not been reported.

Interestingly, the O_{Glu46}–O_{pCA} bond is unusually short, 2.47 Å in the pR_{CW} structure (1.60-Å resolution) [17], which may argue against the presence of an LBHB in the ground state proposed in Ref. [8]. In general, a H-bond donor-acceptor distance can be the shortest when the pK_a difference between donor and acceptor moieties is nearly zero. This is why LBHB and single-well H-bonds are shorter than standard (asymmetric double-well) H-bonds (Figure 1) [11, 20-22]. If the presence of the shorter O_{Glu46}–O_{pCA} bond in the pR_{CW} state relative to the ground state is plausible, this will suggest that "matching pK_a" between the H-bond donor and acceptor moieties is not satisfied in the ground state (at least, less likely than in the pR_{CW} state).

To understand energetics of the unusually short O_{Glu46}–O_{pCA} bond in the pR_{CW} structure, the influence of Tyr42 (i.e, another H-bond partner of *p*CA) on the O_{Glu46}–O_{pCA} H-bond is to be clarified. The LBHB O_{Glu46}–O_{pCA} bond was originally proposed to stabilize "the isolated negative charge" originating from ionized *p*CA in the protein inner core [8]. However, the presence of the polar residue Tyr42 that donates an H bond to *p*CA (O_{Tyr42}–O_{pCA} = 2.50 Å [23] to 2.52 Å [8]) in the ground state appeared to play a role in stabilizing the ionized chromophore (Figure 1) and is possibly an implication that the O_{Glu46}–O_{pCA} bond does not necessarily require characteristics of an LBHB to exist in the protein environment.

On the other hand, in the pR state the presence of the O_{Glu46}–O_{pCA} H bond has been confirmed in spectroscopic studies (e.g., the O_{Glu46}–O_{pCA} H bond is stronger in pR relative to pG [4]), while the presence of the O_{Tyr42}–O_{pCA} is unclear. If the O_{Tyr42}–O_{pCA} H-bond is absent in the pR_{CW} state, pK_a(*p*CA) relative to pK_a(Glu46) is expected to be significantly different from that in the ground state, which can affect the O_{Glu46}–O_{pCA} bond length. Indeed, the O_{Glu46}–O_{pCA} bond is significantly short (2.51 Å) in the Y42F crystal structure [24] relative to the native PYP (2.57 Å [8, 23]). Fourier transform infrared (FTIR) spectroscopic studies also have suggested that the O_{Glu46}–O_{pCA} bond is stronger in the Y42F mutant than in the native PYP [25].

To evaluate how formation of a unusually short H-bond is energetically possible in PYP, we analyzed the H-bond energetics adopting a quantum mechanical/molecular mechanical (QM/MM) approach based on the atomic coordinates of the PYP crystal structures including the pR_{CW} [17] and Y42F [24] structures.

2. COMPUTATIONAL PROCEDURES

QM/MM calculations. The atomic coordinates were taken from the X-ray structures of the native (PDB ID codes 1OT9 or 1OTB) [23] and Y42F (1F9I) [24], PYP proteins and the Laue crystal structure of the pR_{CW} (1TS7) intermediate [17]. To gain better understanding of the electronic structure of the chromophore *p*CA, and the residues in the H-bond network, namely Tyr42, Glu46, Thr50, and Cys69, we performed large-scale QM/MM calculations for the entire PYP protein. Note that the calculated O_{Glu46}–O_{pCA} H-bond length remained unchanged even when Cys69 was involved in the MM region. We employed the so-called electrostatic embedding QM/MM scheme [26] and used the Qsite [27] program code as performed in previous studies [28]. The detailed geometry of QM region was optimized under the influence of MM electrostatic/steric field (see PYP_SI.pdb in SI for geometry). We employed the restricted DFT method with the B3LYP functional and LACVP**+ basis sets. For the QM/MM calculations, we added additional counter ions to neutralize the whole system.

H-bond potential-energy. For following the proton transfer (PT) pathways, we employed an iterative (constrained) QM/MM geometry optimizations with fixing the selected reaction coordinate. First, we prepared for the QM/MM optimized geometry without constraints, and we used the resulting geometry as the initial geometry. Next, the reaction coordinate was defined as a linear combination of two PT distances (O_{donor}–H and H–$O_{acceptor}$). Then, we moved the H atom from the H-bond donor atom (O_{donor}) to the acceptor atom ($O_{acceptor}$) by 0.05 Å, optimized the geometry by constraining the O_{donor}–H and H–$O_{acceptor}$ distances such that the sum of the two distances remained constant in order to really follow the proton motion, and calculated the energy of the resulting geometry at each PT coordinate. This procedure was repeated until the H atom reached the $O_{acceptor}$ atom. Except for the atoms directly involved in the PT reaction coordinate (i.e., O_{donor}, a transferring H, and $O_{acceptor}$ atoms), all of the atomic coordinates in the QM region were fully relaxed (i.e., not fixed) in the generation of the scans.

^{1}H-NMR chemical shift. The NMR chemical shift was calculated by using the GIAOs method [29] implemented in the Qsite [27] and JAGUAR [30] programs. The absolute shielding constant of ^{1}H of tetramethylsilane (TMS) was calculated to be 31.6 ppm on the basis of the atomic coordinates in Ref. [31] and used as the TMS reference for δ_H. We evaluated the accuracy of the quantumchemically calculated δ_H [32]. First, we calculated δ_H for malaete and compounds which are also supposed to contain a strong H bond or an LBHB [33]. The calculated δ_H values are considerably close to the experimentally measured values, with discrepancies of ~1 ppm or less [32]. The discrepancy between the measured values (solution) and the calculated values (solid state) is mainly due to inadequate accounting for the multiconfiguration of the molecular geometry, the proton dynamics, and the ro-vibrational corrections to the nuclear shielding in the calculations. This indicates, however, that the contributions of these features to the values are obviously negligible, which does not practically affect any conclusions from the present study. Hence, the calculated δ_H values should be considered at this level of accuracy [32].

^{1}H-NMR chemical shift validation. The calculated OHO-bond geometries and the NMR chemical shifts can also be evaluated by the correlation proposed by Limbach et al. [34]. The geometric

correlation of the $O_{acceptor}\cdots H–O_{donor}$ bond between the acceptor$\cdots$hydrogen ($O_{acceptor}\cdots H$) distance r_1 and the donor–hydrogen ($O_{donor}–H$) distance r_2 can be obtained by

$$q_2 = 2r^0 + 2q_1 + 2b \ln[1 + \exp(-2q_1/b)],$$

$$b = [2\, q_{2\min} - 2\, r_0]/2 \ln 2,$$

$$q_1 = (r_1 - r_2)/2,$$

$$q_2 = r_1 + r_2, \qquad \text{(eq. 1)}$$

where $q_{2\min}$ represents a minimum value corresponding to the minimum $O_{acceptor}\cdots O_{donor}$ distance in the case of a linear H bond, and r^0 is the equilibrium distance in the fictive free diatomic unit OH [34]. The correlation between the OHO-bond geometry and the ^{1}H NMR chemical shift δ_H can be obtained by

$$\delta_H = \delta_{OH}{}^0 + \Delta_H(4p_1p_2)^m,$$

$$p_1 = \exp[-(q_1 + q_2/2 - r^0)/b],$$

$$p_2 = \exp[-(-q_1 + q_2/2 - r^0)/b], \qquad \text{(eq. 2)}$$

where $\delta_{OH}{}^0$ and Δ_H represent the limiting chemical shifts of the separate fictive groups OH and the excess chemical shift of the quasi-symmetric complex, respectively, and m is an empirical parameter. q_2 is given in eq. 1. Using eqs. (1) and (2), the δ_H can also be obtained, regarding q_2 as the donor–acceptor ($O_{donor}– O_{acceptor}$) distance. We used the same parameters as used in Ref. [34], i.e., $r^0 = 0.93$, $q_{2\min} = 2.36$, $\delta_{OH}{}^0 = 7.9$, $\Delta_H = 13$, and $m = 1.1$, as done in a previous study [32].

3. RESULTS

Influence of Tyr42 on the O_{Glu46}–O_{pCA} bond properties. In the QM/MM geometry, the O_{Glu46}–O_{pCA} bond of 2.51 Å in the Y42F mutant is shorter than the bond of 2.57 Å in the native PYP, in agreement with the crystal structure [24] (Table 2). The calculated δ_H value for the O_{Glu46}–O_{pCA} bond in the Y42F mutant was 16.8 ppm (Table 2), in agreement with a δ_H of 16.7 ppm measured in solution NMR studies [35]. Using the correlation proposed by Limbach et al. [34], an O–O distance of 2.51 Å also predicts a

δ_H of 16.4 ppm, suggesting that the larger δ_H in the Y42F mutant is predominantly due to the decreased O_{Glu46}–O_{pCA} length.

The decrease in the O_{Glu46}–O_{pCA} length upon mutation of Y42F can also be understood from the decrease in the energy near the *p*CA moiety relative to the Glu46 moiety in the potential energy profile (Figure 3), which corresponds to the decrease in the pK_a difference between Glu46 and *p*CA. Thus, the shorter O_{Glu46}–O_{pCA} length in the Y42F mutant with respect to the native PYP is due to pronounced "matching pK_a" between the H-bond donor and acceptor moieties, i.e. the H-bond potential energy shape becomes more symmetric. Similar relationship between the pK_a differences and the H-bond donor-acceptor distances has also been demonstrated for H-bonds in other proteins (e.g., counter ions in bacteriorhodopsin and *Anabaena* sensory rhodopsin [36] and redox active tyrosine D1-Tyr161 in photosystem II [37]).

Such a decrease in the pK_a difference leads to a more symmetrical H bond characteristic of the O_{Glu46}–O_{pCA} bond. According to Frey [13], an essential requirement for a symmetrical H bond is that the proton lies inline with the donor and acceptor atoms; this feature is pronounced in the essentially linear H bond of O_{Glu46}–H–O_{pCA} in the Y42F mutant (172.0°) relative to the that in the native PYP (168.2°) (Table 2). All these features are consistent with previous proposals by Frey et al. [10, 13], Cleland and Kreevoy [9], Schutz and Warshel [11], and Limbach et al. [34]. Note that the resulting properties of the potential-energy curve and δ_H calculated for the present crystal structure of the native PYP (PDB ID code 1OT9, 110 K) are consistent with those previously reported for the other crystal structure (PDB ID code 2ZOH, 295 K) [28, 32].

In summarizing the results, the H-bond donation of Tyr42 to *p*CA contributes to the increase in the O_{Glu46}–O_{pCA} length of the native PYP (2.57 Å) relative to the Y42F mutant (2.51 Å). It should also be noted that the longer O_{Glu46}–O_{pCA} bond in the native PYP does not suggest that the native PYP is energetically unstable relative to the Y42F mutant.

Influence of Tyr42 on the O_{Glu46}–O_{pCA} length in the native PYP. In contrast to the Y42F mutant, it is obvious that Tyr42 donates an H-bond to *p*CA in the ground state of the native PYP [8, 28, 32]. To

investigate the influence of Tyr42 as an H-bond donor to *p*CA on the H-bond network, we performed QM/MM calculations by flipping the hydroxyl group of Tyr42 (i.e., without removing Tyr42). Note that Thr50 is at a H-bond distance with Tyr42 (2.85 Å) in the crystal structure [23] (Table 1).

We found that, if Tyr42 provides an H bond to Thr50, not to *p*CA, the H-bond geometry resulted in an unusually short O_{Glu46}–O_{pCA} bond of 2.46 Å ([short O_{Glu46}–O_{pCA}] bond pattern, Figure 2) with a δ_H of 18.9 ppm, typical values for symmetrical H bonds [13] (Table 1). The potential-energy curve of [short O_{Glu46}–O_{pCA}] resembles that of a single-well H bond as shown in Ref. [20] (Figure 4). The number of H bonds in the chromophore of the [short O_{Glu46}–O_{pCA}] geometry is identical to the [standard] H-bond geometry where Tyr42 provides an H bond to *p*CA (Figure 2). These results demonstrate that Tyr42 in the native PYP is the residue that prevent Glu46 and *p*CA from possessing equal pK_a. A symmetrical H bond is unlikely to form between Glu46 and *p*CA as long as Tyr42 provides an H bond to *p*CA.

Notably, the neutron diffraction geometry (in the ground state) confirmed the presence of an H bond donation from Tyr42 to *p*CA [8], which strongly suggests that in the ground state, O_{Glu46}–O_{pCA} is chemically impossible to form a symmetrical H bond due to the obvious pK_a difference between Glu46 and *p*CA induced by Tyr42. If formation of an LBHB were strongly advantageous, then the hydrogen bond pattern would rearrange to allow formation of an LBHB in the ground state. Hence, to flip the Tyr42 H bond and to form a single-well H bond, a large energy is required (Figure 4), which may be possible only upon photo excitation (discussed later).

Energetics of a single-well H bond. One might consider that the [short O_{Glu46}–O_{pCA}] bond of 2.46 Å with a δ_H of 18.9 ppm is a strong H bond. However, the potential-energy curve of the [short O_{Glu46}–O_{pCA}] bond (QM/MM energy, corresponding to represent not only the energy of the QM region but also contain that of the remaining protein environment) was significantly, energetically high relative to that of the [standard O_{Glu46}–O_{pCA}] bond geometry (Figure 4). The observed chromophore destabilization was mainly due to the loss of O_{Tyr42}–O_{pCA} H bond. The short O_{Glu46}–O_{pCA} bond of 2.46 Å is ~4 kcal/ mol more stabilized than the [standard O_{Glu46}–O_{pCA}] bond of 2.57 Å. However, complete loss of the O_{Tyr42}–O_{pCA} H bond is much more energetically disadvantageous. In addition, it also induces repulsion between

O_{Tyr42} and O_{pCA} (~6 kcal/ mol), destabilizing the chromophore region. (Note; that the corresponding repulsion is absent in the Y42F mutant due to the absence of O_{Tyr42}. Thus, pK_a(*p*CA) is slightly lower than pK_a(Glu46) in the Y42F mutant (Figure 3) in contrast to the [short O_{Glu46}–O_{pCA}] geometry (Figure 4) or the pR_{CW} structure (Figure 5).)

One advantage of the catalytic site of the protein over bulk water is the availability of the preorganized dipoles in the protein environment to stabilize the transition state electrostatically [11, 21]. For enzymes to utilize the protein dipoles effectively in stabilizing the transition state, a larger polarity between the transition state and the protein is energetically advantageous. In the case of PYP, Tyr42 obviously plays a role in providing the corresponding large polarity to the stability of the O_{Glu46}–O_{pCA} bond, which energetically suppresses formation of an LBHB in O_{Glu46}–O_{pCA}. Hence, formation of a short H bond does not necessarily lower the total energy of the protein, as previously reported in other studies [11, 21, 22].

Influence of the H-bond between the carbonyl group of *p*CA and the backbone amide of Cys69 on the O_{Glu46}–O_{pCA} length. The [short O_{Glu46}–O_{pCA}] geometry and the pR_{CW} structure have the same the H-bond patterns of Glu46, *p*CA, and Tyr42, where the O_{Glu46}–O_{pCA} and O_{Tyr42}–O_{pCA} H-bonds are present and absent, respectively (discussed later).

On the other hand, the H-bond between the carbonyl group of *p*CA and the amide group of Cys69, which is present in the the [short O_{Glu46}–O_{pCA}] geometry but absent in the pR_{CW} structure [17]. Irrespective of the difference in the H-bond pattern of Cys69, the O_{Glu46}–O_{pCA} bond lengths are similarly, unusually short in the two structures (Tables 1 and 3). Hence, the presence/absence of the H-bond of Cys69 on the O_{Glu46}–O_{pCA} length appears to be much less crucial to the O_{Glu46}–O_{pCA} bond length than that of Tyr42.

4. DISCUSSION

Presence of a single-well H bond in the pR_{CW} intermediate structure in time-resolved Laue crystallography. The O_{Glu46}–O_{pCA} bond is unusually short, 2.47 Å in the pR_{CW} structure (Table 3).

However, the H atom positions and thus far H-bond pattern are yet not known from the crystal structure. The QM/MM calculations reproduced the unusually short H-bond distance (2.49 Å) on the basis of the pR_{CW} structure only when the [short O_{Glu46}–O_{pCA}] H-bond geometry (Figure 2) was assumed (Table 3). The standard O_{Glu46}–O_{pCA} H-bond geometry (i.e., Tyr42 donates an H bond to *p*CA) yielded the bond length of 2.60 Å even in QM/MM calculations of the pR_{CW} structure. These results confirm that the actual H-bond pattern in the pR_{CW} crystal structure is the [short O_{Glu46}–O_{pCA}] H-bond geometry, where Tyr42 is flipped away from *p*CA, rather than the [standard O_{Glu46}–O_{pCA}] H-bond geometry, where Tyr donates an H bond to *p*CA.

The existence of the unusually short H-bond appears to be plausible not only in the pR_{CW} structure [17], but also in the pR species [14-16] observed in spectroscopic studies. FTIR studies have suggested that the H bond between Glu46 and *p*CA becomes stronger in pR relative to pG as suggested by the downshift in the C=O stretching frequency of protonated Glu46 [4]. Because shortening a H-bond donor and acceptor distance leads to migration of the H atom toward the acceptor moiety (e.g., Ref. [32, 36]), the observed downshift in the C=O stretching frequency of Glu46 is consistent with the presence of the unusually short O_{Glu46}–O_{pCA} bond in the pR_{CW} structure. Significance of the H-bond pattern of Tyr42 and *p*CA in the O_{Glu46}–O_{pCA} length can also be seen in studies of the Y42F mutant; (i) the Y42F crystal structure [24] has a shorter O_{Glu46}–O_{pCA} bond than the native PYP (Table 2) and (ii) the C=O stretching frequency of protonated Glu46 in the Y42F mutant is downshifted relative to the wild type PYP in FTIR studies [25].

Interestingly, the potential-energy curve of the O_{Glu46}–O_{pCA} bond (2.49 Å) in the pR_{CW} crystal structure resembles that of a typical single-well H bond; the barrierless potential for the PT is an indication of the pR_{CW} intermediate being ready for the PT (Figure 5). In FTIR studies, the C=O stretching frequency for protonated Glu46 is downshifted to 1732 cm^{-1} in pR relative to 1740 cm^{-1} in pG, suggesting that the H atom in the O_{Glu46}–O_{pCA} bond (i) remains in the Glu46 moiety (i.e. can interact with Glu46) but simultaneously (ii) significantly migrated toward the *p*CA moiety [4]; this is exactly the case for a single-well H bond. Indeed, in FTIR studies the existence of a single-well H-bond

has been already proposed [4]; a stronger H-bond in pR relative to pG lowers the energy barrier for proton transfer from Glu46 to *p*CA (see also Figure 4 in Ref. [4]). The present study confirms this, by demonstrating that the unusually short H-bond in the pR_{CW} crystal structure [17] is reproducible on the basis of quantum chemistry. Note that the O_{Glu46}–O_{pCA} H bond is absent in the pB state [4] and solution structures of the pB state [18].

If the short O_{Glu46}–O_{pCA} H bond could be a very strong bond, the pR_{CW} intermediate would be very stable and the proceeding pB state would never form in such a time scale. It should also be noted that a lifetime of hundreds μs for the pR_{CW} state is due to the large structural change rather than the PT from Glu46 to *p*CA. In addition, in a single-well H-bond, movement of a proton between the donor and acceptor moieties is not directly associated with breakage of the H-bond. (note, the potential energy profile of a single-well H-bond only suggests that movement of a proton is easier than in a standard H-bond due to the absence of the energy barrier.) Breakage of the short O_{Glu46}–O_{pCA} H bond can occur as a result of the large structural change, which is driven by the photon energy stored in the system [38]. Hence, the pR intermediate can lower the energy to proceed the pB state by abolishing the unusually short O_{Glu46}–O_{pCA} H bond of <2.5 Å.

Here, one may also rediscover the so-called "principle of frustration", where in the folding process, proteins (may not completely eliminate but at least) need to minimize frustration [39]. In terms of the "local" H-bond network of *p*CA, formation of the unusually short H-bond is energetically allowed (or favored) at the stage of the pR intermediate. However, this is not the energetically lowest state of the "entire" protein, which can also be understood by pR being followed by pB.

5. CONCLUDING REMARKS

The presence of the shorter O_{Glu46}–O_{pCA} bond (2.47 Å) in the pR_{CW} crystal structure [17] relative to the ground state structure (2.57 Å) indicates that the "equal pK_a" requirement for formation of a single-well H-bond is satisfied in the pR_{CW} intermediate, but not in the ground state. If matching pK_a were satisfied in the ground state, the O_{Glu46}–O_{pCA} bond (~2.6 Å [8, 23]) could neither be further shorten to

~2.5 Å in the pR_{CW} structure [17] nor become stronger in pR as observed in FTIR studies [4]. An LBHB or a single-well H-bond is less likely to form between Glu46 and *p*CA as long as Tyr42 provides an H bond to *p*CA in the native PYP.

The present case clearly shows that the formation of a short symmetrical H bond does not necessarily help to decrease the total energy of the active site. Comparison of the energetics of the two possible H-bond patterns in the same protein unambiguously enabled us to realize that merely focusing on a short H bond might lead to neglect of the total energy.

6. ACKNOWLEDGMENT

This research was supported by the JST PRESTO program (K.S. and H.I), Grant-in-Aid for Scientific Research from the Ministry of Education, Culture, Sports, Science and Technology (MEXT) of Japan (22740276 to K.S.), Special Coordination Fund for Promoting Science and Technology of MEXT (H.I), Takeda Science Foundation (H.I.), Kyoto University Step-up Grant-in-Aid for young scientists (H.I.), and Grant for Basic Science Research Projects from The Sumitomo Foundation (H.I.).

7. REFERENCES

[1] W.W. Sprenger, W.D. Hoff, J.P. Armitage and K.J. Hellingwerf, The eubacterium *Ectothiorhodospira halophila* is negatively phototactic, with a wavelength dependence that fits the absorption spectrum of the photoactive yellow protein, J Bacteriol 175 (1993) 3096-104.

[2] M. Baca, G.E. Borgstahl, M. Boissinot, P.M. Burke, D.R. Williams, K.A. Slater and E.D. Getzoff, Complete chemical structure of photoactive yellow protein: novel thioester-linked 4-hydroxycinnamyl chromophore and photocycle chemistry, Biochemistry 33 (1994) 14369-14377.

[3] M. Kim, R.A. Mathies, W.D. Hoff and K.J. Hellingwerf, Resonance Raman evidence that the thioester-linked 4-hydroxycinnamyl chromophore of photoactive yellow protein is deprotonated, Biochemistry 34 (1995) 12669-12672.

[4] A. Xie, W.D. Hoff, A.R. Kroon and K.J. Hellingwerf, Glu46 donates a proton to the 4-hydroxycinnamate anion chromophore during the photocycle of photoactive yellow protein, Biochemistry 35 (1996) 14671-14678.

[5] E. Demchuk, U.K. Genick, T.T. Woo, E.D. Getzoff and D. Bashford, Protonation states and pH titration in the photocycle of photoactive yellow protein, Biochemistry 39 (2000) 1100-13.

[6] G.E. Borgstahl, D.R. Williams and E.D. Getzoff, 1.4 Å structure of photoactive yellow protein, a cytosolic photoreceptor: unusual fold, active site, and chromophore, Biochemistry 34 (1995) 6278-6287.

[7] E.D. Getzoff, K.N. Gutwin and U.K. Genick, Anticipatory active-site motions and chromophore distortion prime photoreceptor PYP for light activation, Nat Struct Biol 10 (2003) 663-668.

[8] S. Yamaguchi, H. Kamikubo, K. Kurihara, R. Kuroki, N. Niimura, N. Shimizu, Y. Yamazaki and M. Kataoka, Low-barrier hydrogen bond in photoactive yellow protein, Proc Natl Acad Sci U S A 106 (2009) 440-444.

[9] W.W. Cleland and M.M. Kreevoy, Low-barrier hydrogen bonds and enzymic catalysis, Science 264 (1994) 1887-1890.

[10] P.A. Frey, S.A. Whitt and J.B. Tobin, A low-barrier hydrogen bond in the catalytic triad of serine proteases, Science 264 (1994) 1927-30.

[11] C.N. Schutz and A. Warshel, The low barrier hydrogen bond (LBHB) proposal revisited: the case of the Asp... His pair in serine proteases, Proteins 55 (2004) 711-723.

[12] G.A. Jeffrey, An Introduction to Hydrogen Bonding (1997) Oxford University Press, Oxford.

[13] P.A. Frey, in Isotope Effects in Chemistry and Biology (Kohen, A. and Limbach, H.-H., Eds.) (2006) pp 975-993, CRC press, Boca Raton, FL.

[14] W.D. Hoff, I.H. van Stokkum, H.J. van Ramesdonk, M.E. van Brederode, A.M. Brouwer, J.C. Fitch, T.E. Meyer, R. van Grondelle and K.J. Hellingwerf, Measurement and global analysis of the absorbance changes in the photocycle of the photoactive yellow protein from Ectothiorhodospira halophila, Biophys J 67 (1994) 1691-705.

[15] L. Ujj, S. Devanathan, T.E. Meyer, M.A. Cusanovich, G. Tollin and G.H. Atkinson, New photocycle intermediates in the photoactive yellow protein from Ectothiorhodospira halophila: picosecond transient absorption spectroscopy, Biophys J 75 (1998) 406-12.

[16] M. Unno, M. Kumauchi, N. Hamada, F. Tokunaga and S. Yamauchi, Resonance Raman evidence for two conformations involved in the L intermediate of photoactive yellow protein, J Biol Chem 279 (2004) 23855-8.

[17] H. Ihee, S. Rajagopal, V. Srajer, R. Pahl, S. Anderson, M. Schmidt, F. Schotte, P.A. Anfinrud, M. Wulff and K. Moffat, Visualizing reaction pathways in photoactive yellow protein from nanoseconds to seconds, Proc Natl Acad Sci U S A 102 (2005) 7145-50.

[18] C. Bernard, K. Houben, N.M. Derix, D. Marks, M.A. van der Horst, K.J. Hellingwerf, R. Boelens, R. Kaptein and N.A. van Nuland, The solution structure of a transient photoreceptor intermediate: Delta25 photoactive yellow protein, Structure 13 (2005) 953-62.

[19] E.C. Carroll, S.H. Song, M. Kumauchi, I.H. van Stokkum, A. Jailaubekov, W.D. Hoff and D.S. Larsen, Subpicosecond Excited-State Proton Transfer Preceding Isomerization During the Photorecovery of Photoactive Yellow Protein, J Phys Chem Lett 1 (2010) 2793-2799.

[20] C.L. Perrin and J.B. Nielson, "Strong" hydrogen bonds in chemistry and biology, Annu Rev Phys Chem 48 (1997) 511-544.

[21] A. Warshel, A. Papazyan and P.A. Kollman, On low-barrier hydrogen bonds and enzyme catalysis, Science 269 (1995) 102-106.

[22] C.L. Perrin, Are short, low-barrier hydrogen bonds unusually strong?, Acc Chem Res 43 (2010) 1550-1557.

[23] S. Anderson, S. Crosson and K. Moffat, Short hydrogen bonds in photoactive yellow protein, Acta Crystallogr D Biol Crystallogr 60 (2004) 1008-1016.

[24] R. Brudler, T.E. Meyer, U.K. Genick, S. Devanathan, T.T. Woo, D.P. Millar, K. Gerwert, M.A. Cusanovich, G. Tollin and E.D. Getzoff, Coupling of hydrogen bonding to chromophore conformation and function in photoactive yellow protein, Biochemistry 39 (2000) 13478-86.

[25] C.P. Joshi, H. Otto, D. Hoersch, T.E. Meyer, M.A. Cusanovich and M.P. Heyn, Strong hydrogen bond between glutamic acid 46 and chromophore leads to the intermediate spectral form and excited state proton transfer in the Y42F mutant of the photoreceptor photoactive yellow protein, Biochemistry 48 (2009) 9980-93.

[26] A. Warshel and M. Levitt, Theoretical studies of enzymic reactions: dielectric, electrostatic and steric stabilization of the carbonium ion in the reaction of lysozyme, J. Mol. Biol. 103 (1976) 227-249.

[27] QSite, version 5.8, Schrödinger, LLC, New York, NY, 2012.

[28] K. Saito and H. Ishikita, Energetics of short hydrogen bonds in photoactive yellow protein, Proc Natl Acad Sci U S A 109 (2012) 167-172.

[29] Y. Cao, M.D. Beachy, D.A. Braden, L. Morrill, M.N. Ringnalda and R.A. Friesner, Nuclear-magnetic-resonance shielding constants calculated by pseudospectral methods, J Chem Phys 122 (2005) 224116.

[30] Jaguar, version 7.5, Schrödinger, LLC, New York, NY, 2008.

[31] A.K. Wolf, J. Glinnemann, L. Fink, E. Alig, M. Bolte and M.U. Schmidt, Predicted crystal structures of tetramethylsilane and tetramethylgermane and an experimental low-temperature structure of tetramethylsilane, Acta Crystallogr B 66 (2010) 229-36.

[32] K. Saito and H. Ishikita, H atom positions and nuclear magnetic resonance chemical shifts of short H bonds in photoactive yellow protein, Biochemistry 51 (2012) 1171-7.

[33] F. Hibbert and J. Emsley, Hydrogen bonding and chemical reactivity, Adv. Phys. Org. Chem. 26 (1990) 255-379.

[34] H.-H. Limbach, P.M. Tolstoy, N. Pérez-Hernández, J. Guo, I.G. Shenderovich and G.S. Denisov, OHO hydrogen bond geometries and NMR chemical shifts: from equilibrium structures to geometric H/D isotope effects, with applications for water, protonated water, and compressed ice, Isr J Chem 49 (2009) 199-216.

[35] P.A. Sigala, M.A. Tsuchida and D. Herschlag, Hydrogen bond dynamics in the active site of photoactive yellow protein, Proc Natl Acad Sci U S A 106 (2009) 9232-7.

[36] K. Saito, H. Kandori and H. Ishikita, Factors that differentiate the H-bond strengths of water near the Schiff bases in bacteriorhodopsin and *Anabaena* sensory rhodopsin, J Biol Chem (2012) 34009-18.

[37] K. Saito, J.-R. Shen, T. Ishida and H. Ishikita, Short hydrogen-bond between redox-active tyrosine Y_Z and D1-His190 in the photosystem II crystal structure, Biochemistry 50 (2011) 9836-9844.

[38] M.E. van Brederode, T. Gensch, W.D. Hoff, K.J. Hellingwerf and S.E. Braslavsky, Photoinduced volume change and energy storage associated with the early transformations of the photoactive yellow protein from Ectothiorhodospira halophila, Biophys J 68 (1995) 1101-9.

[39] H. Nymeyer, A.E. Garcia and J.N. Onuchic, Folding funnels and frustration in off-lattice minimalist protein landscapes, Proc Natl Acad Sci U S A 95 (1998) 5921-8.

[40] T. Matsui, T. Baba, K. Kamiya and Y. Shigeta, An accurate density functional theory based estimation of pK(a) values of polar residues combined with experimental data: from amino acids to minimal proteins, Phys Chem Chem Phys 14 (2012) 4181-7.

[41] S. Hammes-Schiffer, Theoretical perspectives on proton-coupled electron transfer reactions, Acc Chem Res 34 (2001) 273-81.

FIGURE CAPTIONS

Figure 1. (a) Overview of typical potential-energy profiles: (top) standard H-bonds (asymmetric double-well), typically with an O_{donor}–$O_{acceptor}$ distance >~2.6 Å; (middle) low barrier H-bond (LBHB), typically with an O_{donor}–$O_{acceptor}$ distance of 2.5–2.6 Å; (bottom) single-well (ionic) H-bonds, typically with an O_{donor}–$O_{acceptor}$ distance of <~2.5 Å [20].

(b) H atom positions of the O_{Glu46}–O_{pCA} bond (left) in the neutron diffraction analysis (green sphere, PDB ID code 2ZOI) [8]. (right) QM/MM optimized structure based on the X-ray crystal structure (cyan sphere, PDB ID code 1OT9) [23].

Figure 2. Possible H-bond patterns in the native PYP. QM/MM optimized geometries of (left) the [standard] and (right) [short O_{Glu46}–O_{pCA}] H-bond patterns.

Figure 3. Energy profiles along the proton transfer coordinate for the O_{Glu46}–O_{pCA} bond in the native PYP (black curve) and the Y42F mutant (red curve). Changes of the properties induced by the Y42F mutation are indicated by open arrows. For comparison, the energy minimum was set to zero for both the native PYP and the Y42F mutant. Although pK_a should refer to free energy rather than energy, it can be practically assumed to result in the same tendency [40], in particular for the case with short H bonds where the proton motion is considerably restricted due to the presence of the donor and acceptor moieties in the protein environment. Note that pK_a is not for a proton release from the O_{donor}–H…$O_{acceptor}$ bond (i.e., pK_a([O_{donor}–H…$O_{acceptor}$]/[O_{donor}…$O_{acceptor}$]$^-$), but pK_a([O_{donor}–H]/[O_{donor}]$^-$) and pK_a([$O_{acceptor}$–H]/[$O_{acceptor}$]$^-$) for each diabatic potential curve of the donor/acceptor moiety [41].

Figure 4. Energy profiles along the proton transfer coordinate for the O_{Glu46}–O_{pCA} bond in the [standard] H-bond geometry (black curve) and the short O_{Glu46}–O_{pCA} bond geometry (blue) in the native PYP. The two H-bond patterns differ predominantly at the H atom (red) orientation of Tyr42. The open arrows indicate a reorientation of the hydroxyl H atom of Tyr42, which separates the two H-bond geometries energetically. Note that the atomic coordinates of Tyr42 were fully relaxed (not fixed) in each QM/MM calculation. The energy minimum of the [standard] H-bond geometry was set to zero.

The two energy profiles describe the total QM/MM energy of the entire system, including both QM and MM regions.

Figure 5. Energy profiles along the proton transfer coordinate for the O_{Glu46}–O_{pCA} bond in the pRcw intermediate (PDB ID code 1TS7).

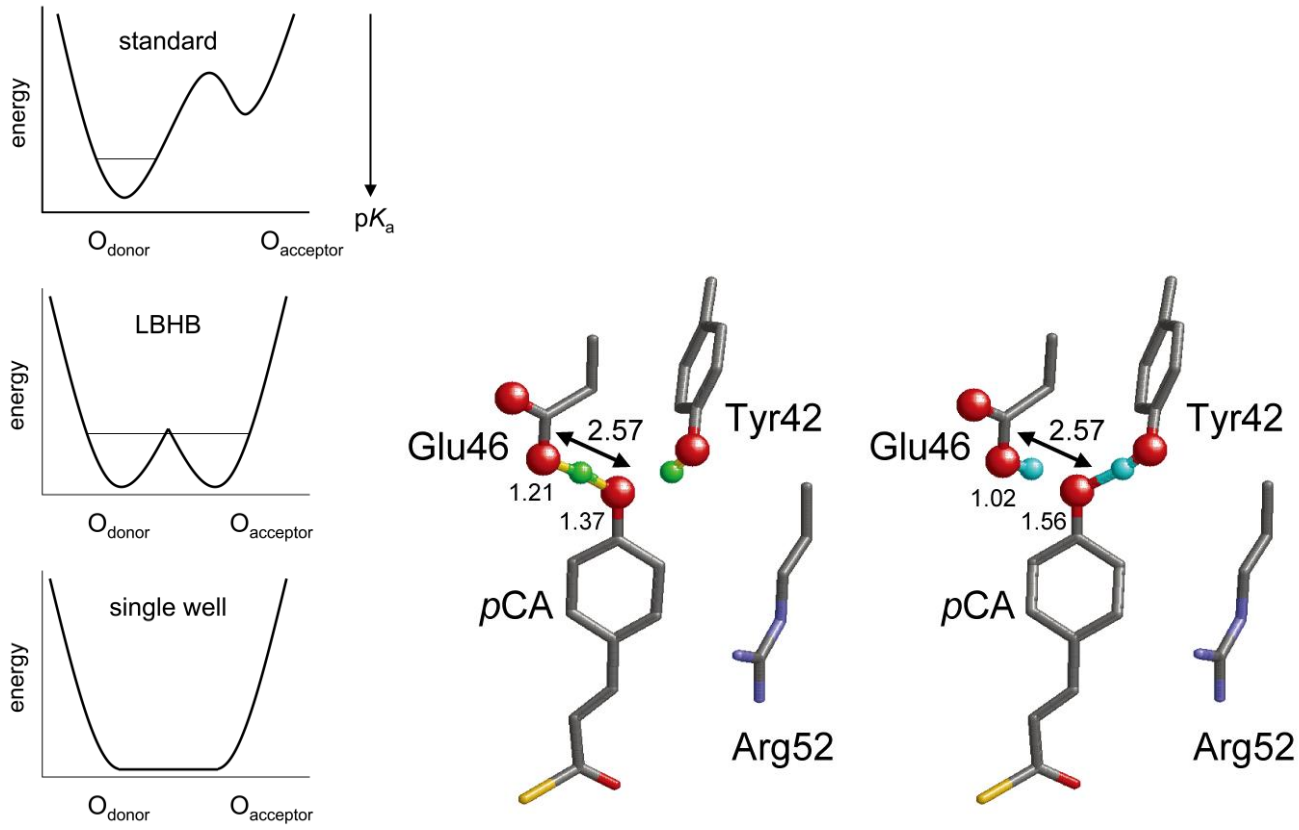
standard
energy
pKa
Odonor
Oacceptor
LBHB
energy
Odonor
Oacceptor
single well
energy
Odonor
Oacceptor
Glu46
2.57
Tyr42
1.21
1.37
pCA
Arg52
Glu46
2.57
Tyr42
1.02
1.56
pCA
Arg52

(a) (b)

Figure 1.

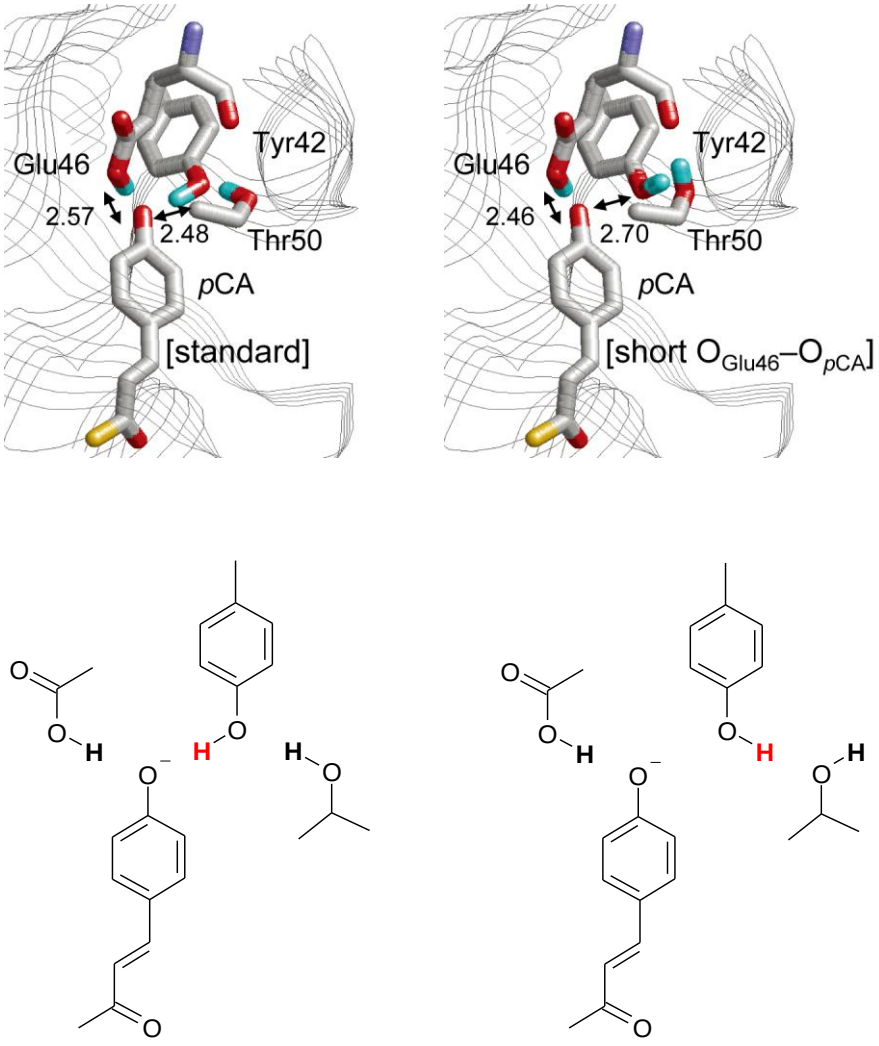
Glu46
Tyr42
2.57
2.48
Thr50
pCA
[standard]
Glu46
Tyr42
2.46
2.70
Thr50
pCA
[short O$_{Glu46}$–O$_{pCA}$]

Figure 2.

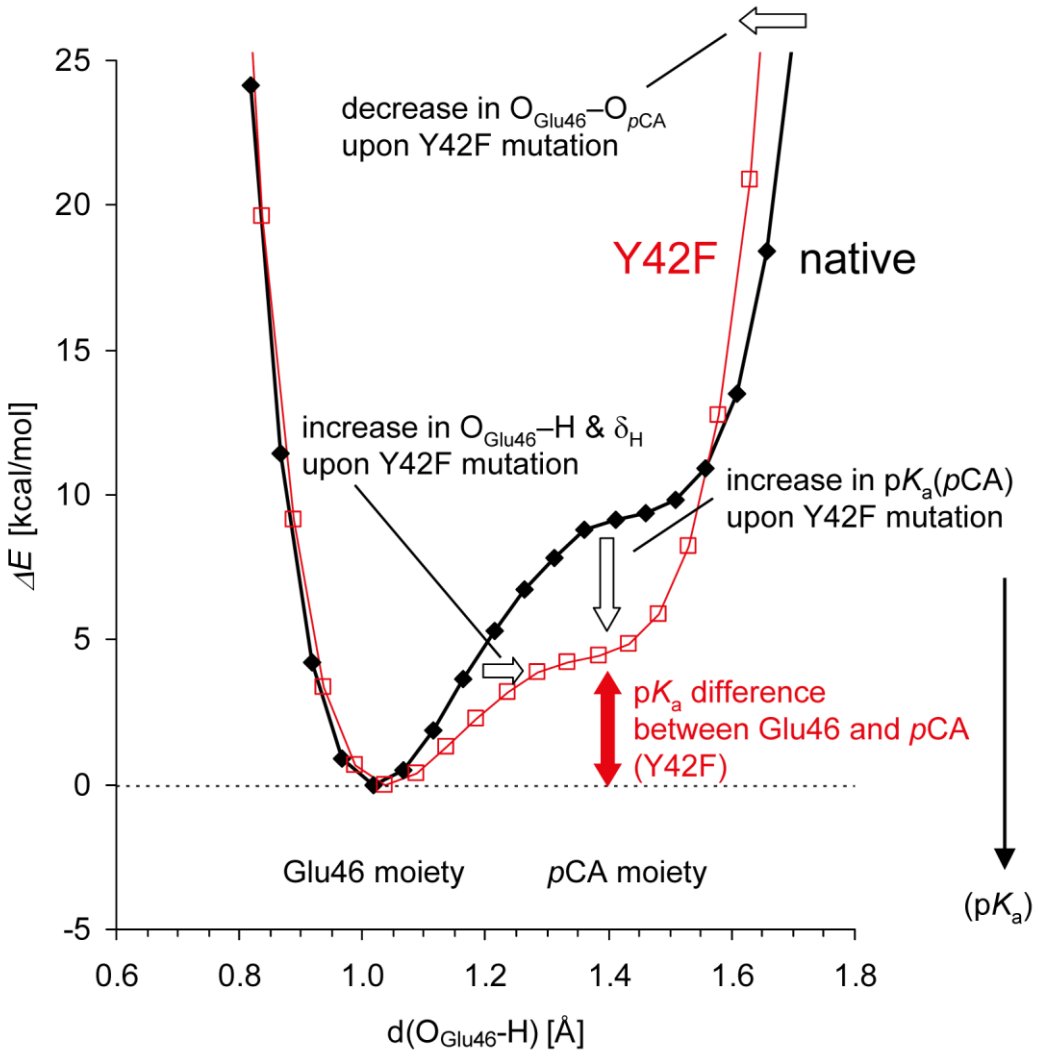
decrease in O_{Glu46}–O_{pCA}
upon Y42F mutation
Y42F
native
increase in O_{Glu46}–H & δ_H
upon Y42F mutation
increase in pK_a(*p*CA)
upon Y42F mutation
pK_a difference
between Glu46 and *p*CA
(Y42F)
Glu46 moiety
*p*CA moiety
(pK_a)
ΔE [kcal/mol]
d(O_{Glu46}-H) [Å]
25
20
15
10
5
0
-5
0.6
0.8
1.0
1.2
1.4
1.6
1.8

Figure 3.

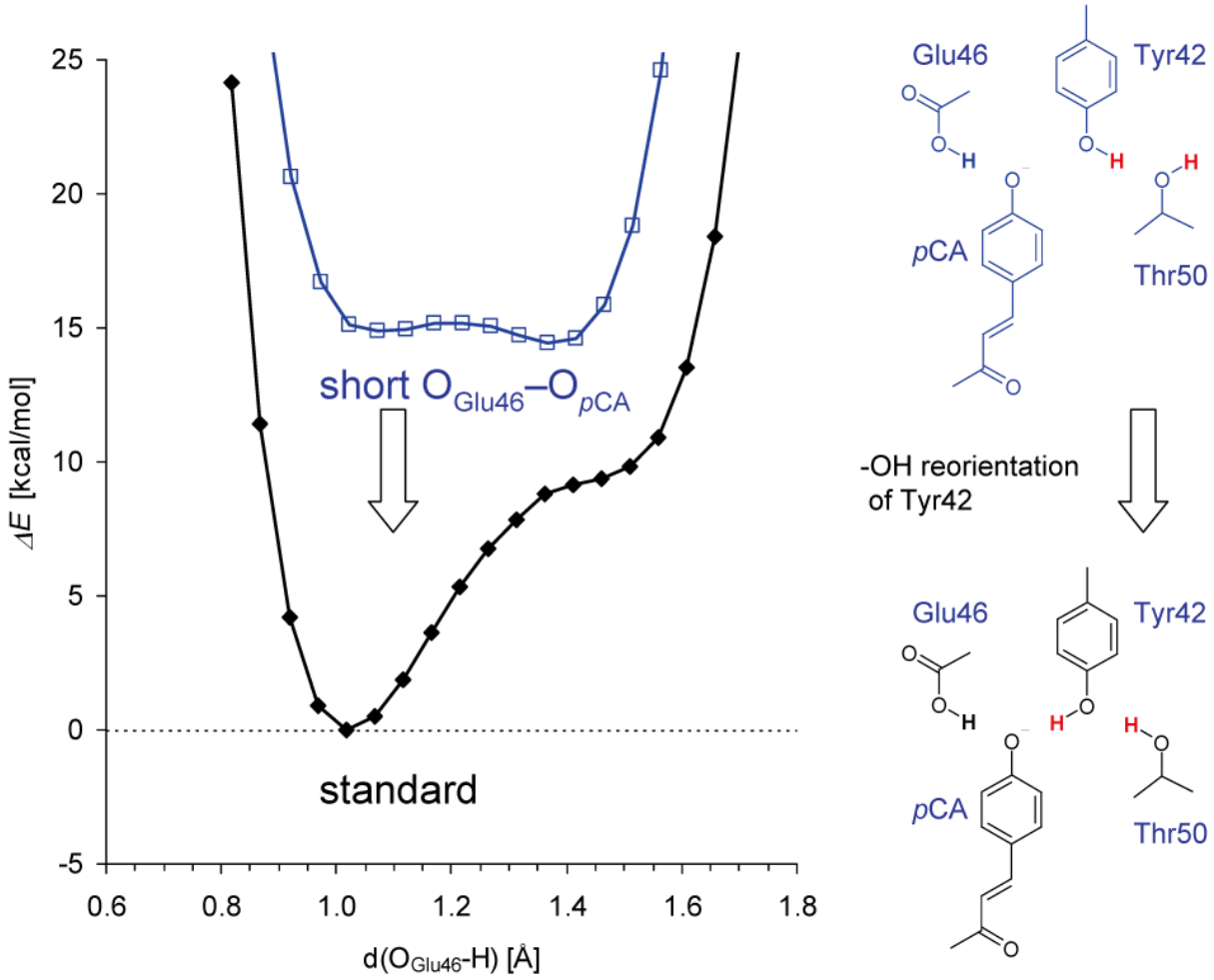
25
20
15
10
5
0
-5
ΔE [kcal/mol]
0.6
0.8
1.0
1.2
1.4
1.6
1.8
d(O Glu46-H) [Å]
short O Glu46–O pCA
standard
Glu46
Tyr42
pCA
Thr50
-OH reorientation
of Tyr42
Glu46
Tyr42
pCA
Thr50

Figure 4.

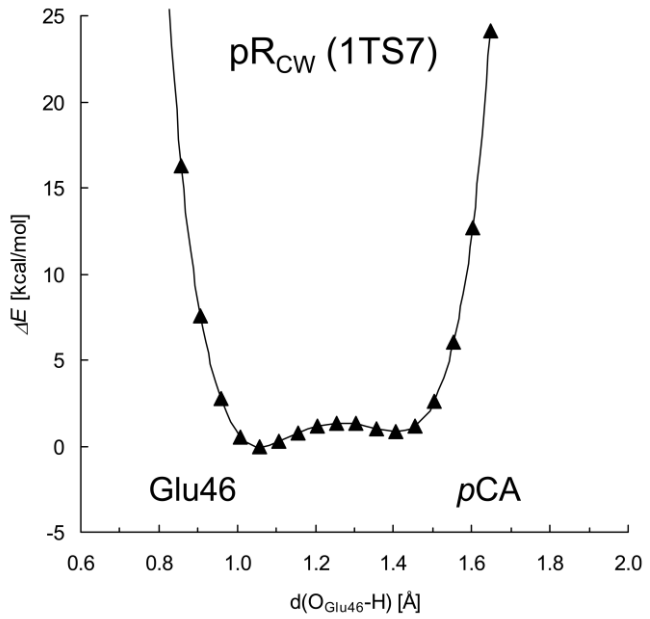
pR$_{CW}$ (1TS7)
ΔE [kcal/mol]
25
20
15
10
5
0
-5
0.6
0.8
1.0
1.2
1.4
1.6
1.8
2.0
Glu46
pCA
d(O$_{Glu46}$-H) [Å]

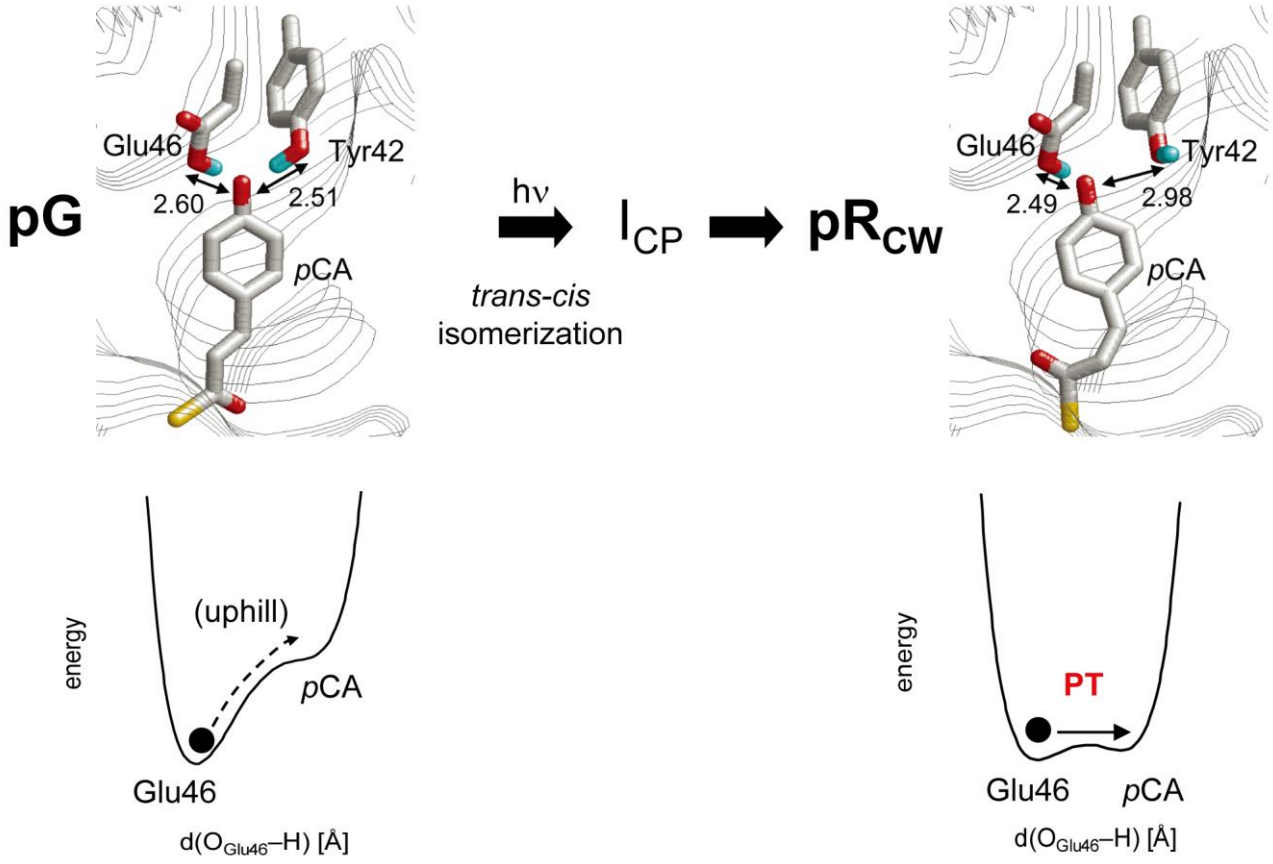
pG
Glu46
Tyr42
2.60
2.51
pCA
hν
trans-cis
isomerization
I$_{CP}$
pR$_{CW}$
Glu46
Tyr42
2.49
2.98
pCA
energy
(uphill)
pCA
Glu46
d(O$_{Glu46}$–H) [Å]
energy
PT
Glu46
pCA
d(O$_{Glu46}$–H) [Å]

Figure 5.

Table 1. (i) Experimental and calculated geometries (in angstrom for distance and degree for angle) and (ii) δ_H (in ppm) of the native PYP. For the complete atomic coordinates of the QM/MM geometries, see PYP_SI.pdb in SI. n.d.; not determined. The error in O–O distance in the crystal was estimated to be 0.01–0.02 Å [23].

(i)

	Native		
	1OT9	**calc.**	**calc.**
[geometry]		standard	short O_{Glu46}–O_{pCA}
O_{Glu46}–O_{pCA}	2.59	2.57	**2.46**
O_{Glu46}–H	n.d.	1.02	1.07
H–O_{pCA}	n.d.	1.56	1.39
(O_{Glu46}–H–O_{pCA})	n.d.	168.2	169.9
O_{Tyr42}–O_{pCA}	2.50	2.48	2.70
O_{Tyr42}–H	n.d.	1.02	0.97
H–O_{pCA}	n.d.	1.47	3.20
(O_{Tyr42}–H–O_{pCA})	n.d.	170.9	51.1
O_{Thr50}–O_{Tyr42}	2.85	2.79	2.86
O_{Thr50}–$O_{C=O, 46}$	3.13	3.08	2.81
O_{Thr50}–O_{pCA}	4.02	4.01	4.09

[a] See Ref. [35].

(ii)

		standard	**short O_{Glu46}–O_{pCA}**
	solution	**calc.**	**calc.**
Glu46	15.2[a]	14.8	18.8
Tyr42	13.7[a]	14.9	5.7

Table 2. (i) Experimental and calculated geometries (in angstrom for distance and degree for angle) and (ii) δ_H (in ppm) of the mutant PYP proteins. Values for the native PYP with the [standard] H-bond pattern are also shown for comparison. For the complete atomic coordinates of the QM/MM geometries, see PYP_SI.pdb in SI. n.d.; not determined.

(i)

	native		**Y42F**	
	crystal (1OT9)	**calc.**	**crystal (1F9I)**	**calc.**
O_{Glu46}–O_{pCA}	2.59	2.57	**2.51**	**2.50**
O_{Glu46}–H	n.d.	1.02	n.d.	1.04
H–O_{pCA}	n.d.	1.56	n.d.	1.47
(O_{Glu46}–H–O_{pCA})	n.d.	168.2	n.d.	172.0
O_{Tyr42}–O_{pCA}	2.50	2.48	n.d.	n.d.
O_{Tyr42}–H	n.d.	1.02	n.d.	n.d.
H–O_{pCA}	n.d.	1.47	n.d.	n.d.
(O_{Tyr42}–H–O_{pCA})	n.d.	170.9	n.d.	n.d.
O_{Thr50}–O_{Tyr42}	2.85	2.79	n.d.	n.d.
O_{Thr50}–$O_{C=O, 46}$	3.13	3.08	3.23	3.22
O_{Thr50}–O_{pCA}	4.02	4.01	2.79	2.76

[a] See Ref. [35].

(ii)

	native		**Y42F**	
	solution	**calc.**	**solution**	**calc.**
Glu46	15.2[a]	14.8	16.7[a]	16.8
Tyr42	13.7[a]	14.9	n.d.	n.d.

[a] See Ref. [35].

Table 3. Experimental and calculated geometries (in angstrom for distance and degree for angle) of the pRCW intermediate identified in time-resolved Laue crystallography [17]. Values for the native PYP with the [standard] H-bond pattern are also shown for comparison. For the complete atomic coordinates of the QM/MM geometries, see PYP_SI.pdb in SI. n.d.; not determined.

	Dark		**pR_{CW}**		
	1OTB	**calc.**	**1TS7**	**calc.**	**calc.**
[geometry]		standard		short O_{Glu46}–O_{pCA}	standard
O_{Glu46}–O_{pCA}	2.58	2.60	**2.47**	**2.49**	2.60
O_{Glu46}–H	n.d.	1.02	n.d.	1.06	1.02
H–O_{pCA}	n.d.	1.59	n.d.	1.43	1.59
(O_{Glu46}–H–O_{pCA})	n.d.	170.1	n.d.	172.7	171.2
O_{Tyr42}–O_{pCA}	2.51	2.51	2.83	2.98	2.55
O_{Tyr42}–H	n.d.	1.02	n.d.	0.97	1.02
H–O_{pCA}	n.d.	1.50	n.d.	n.d.	1.53
(O_{Tyr42}–H–O_{pCA})	n.d.	170.3	n.d.	n.d.	174.9
O_{Thr50}–O_{Tyr42}	2.89	2.84	2.83	2.83	2.89
O_{Thr50}–$O_{C=O,\ 46}$	3.17	3.05	3.38	2.74	3.24

[a] See Ref. [35].

TITLE SUPPORTING INFOMATION FOR:
TITLE 2 FORMATION OF A UNUSUALLY SHORT HYDROGEN BOND IN PHOTOACTIVE YELLOW PROTEIN
TITLE 3
TITLE 4 K.SAITO,H.ISHIKITA
REMARK 400
REMARK 400 TABLE OF CONTENTS
REMARK 400 GEOMETREIS OF QM REGION IN TABLE 1(MODEL 1-2)
REMARK 400 GEOMETREIS OF QM REGION IN TABLE 2(MODEL 3)
REMARK 400 GEOMETREIS OF QM REGION IN TABLE 3(MODEL 4-6)
REMARK 400
REMARK 400
REMARK 400 TABLE 1
REMARK 400 MODEL 1:NATIVE(1OT9)/STANDARD
REMARK 400 MODEL 2:NATIVE(1OT9)/SHORT O_GLU46-O_PCA
REMARK 400
REMARK 400 TABLE 2
REMARK 400 MODEL 3:Y42F(1F9I)
REMARK 400
REMARK 400 TABLE 3
REMARK 400 MODEL 4:NATIVE(1OTB)/STANDARD
REMARK 400 MODEL 5:PRCW(1TS7)/SHORT O_GLU46-O_PCA
REMARK 400 MODEL 6:PRCW(1TS7)/STANDARD
REMARK 400
MODEL 1
ATOM 1 CB TYR A 42 15.209 -19.515 5.290 1.00 6.58 ACHN C
ATOM 2 CG TYR A 42 14.475 -18.203 5.419 1.00 5.70 ACHN C
ATOM 3 CD1 TYR A 42 15.165 -16.984 5.469 1.00 6.28 ACHN C
ATOM 4 CD2 TYR A 42 13.084 -18.171 5.562 1.00 5.86 ACHN C
ATOM 5 CE1 TYR A 42 14.509 -15.774 5.671 1.00 6.24 ACHN C
ATOM 6 CE2 TYR A 42 12.403 -16.967 5.742 1.00 5.54 ACHN C
ATOM 7 CZ TYR A 42 13.117 -15.763 5.792 1.00 5.87 ACHN C
ATOM 8 OH TYR A 42 12.462 -14.570 5.928 1.00 6.38 ACHN O
ATOM 9 1HB TYR A 42 16.057 -19.557 5.981 1.00 0.00 ACHN H
ATOM 10 2HB TYR A 42 14.526 -20.315 5.575 1.00 0.00 ACHN H
ATOM 11 HD1 TYR A 42 16.237 -16.990 5.326 1.00 0.00 ACHN H
ATOM 12 HD2 TYR A 42 12.519 -19.098 5.536 1.00 0.00 ACHN H
ATOM 13 HE1 TYR A 42 15.062 -14.843 5.714 1.00 0.00 ACHN H
ATOM 14 HE2 TYR A 42 11.322 -16.951 5.824 1.00 0.00 ACHN H
ATOM 15 HH TYR A 42 11.518 -14.700 5.560 1.00 0.00 ACHN H
ATOM 16 CB GLU A 46 14.163 -14.908 1.908 1.00 5.29 ACHN C
ATOM 17 CG GLU A 46 12.774 -14.903 2.565 1.00 5.41 ACHN C
ATOM 18 CD GLU A 46 11.661 -14.222 1.784 1.00 5.62 ACHN C
ATOM 19 OE1 GLU A 46 11.830 -13.668 0.707 1.00 7.37 ACHN O
ATOM 20 OE2 GLU A 46 10.449 -14.222 2.337 1.00 6.10 ACHN O
ATOM 21 1HB GLU A 46 14.850 -15.492 2.526 1.00 0.00 ACHN H
ATOM 22 2HB GLU A 46 14.107 -15.409 0.939 1.00 0.00 ACHN H
ATOM 23 1HG GLU A 46 12.798 -14.439 3.555 1.00 0.00 ACHN H
ATOM 24 2HG GLU A 46 12.474 -15.935 2.762 1.00 0.00 ACHN H
ATOM 25 HE2 GLU A 46 10.422 -14.580 3.289 1.00 0.00 ACHN H
ATOM 26 CB THR A 50 11.521 -10.954 5.479 1.00 6.77 ACHN C
ATOM 27 OG1 THR A 50 12.574 -11.784 5.963 1.00 6.60 ACHN O
ATOM 28 CG2 THR A 50 10.888 -11.404 4.161 1.00 7.11 ACHN C
ATOM 29 HB THR A 50 10.699 -10.961 6.219 1.00 0.00 ACHN H
ATOM 30 HG1 THR A 50 12.524 -12.714 5.672 1.00 0.00 ACHN H
ATOM 31 1HG2 THR A 50 11.585 -11.450 3.322 1.00 0.00 ACHN H
ATOM 32 2HG2 THR A 50 10.062 -10.734 3.896 1.00 0.00 ACHN H
ATOM 33 3HG2 THR A 50 10.464 -12.398 4.282 1.00 0.00 ACHN H
ATOM 34 SG CYS A 69 2.114 -11.220 6.330 1.00 6.37 ACHN S
TER 35 CYS A 69
HETATM 36 C1 PCA 169 3.506 -11.789 7.322 1.00 6.48 COFA C
HETATM 37 O1 PCA 169 3.446 -12.037 8.523 1.00 7.12 COFA O
HETATM 38 C2 PCA 169 4.701 -11.982 6.533 1.00 6.31 COFA C

```
HETATM   39  C3  PCA   169       5.870 -12.315   7.148  1.00  6.56      COFA C
HETATM   40  C1P PCA   169       7.027 -12.886   6.531  1.00  5.76      COFA C
HETATM   41  C2P PCA   169       8.164 -13.207   7.301  1.00  6.08      COFA C
HETATM   42  C3P PCA   169       9.250 -13.861   6.751  1.00  6.45      COFA C
HETATM   43  C4P PCA   169       9.241 -14.239   5.379  1.00  5.49      COFA C
HETATM   44  C5P PCA   169       8.079 -13.951   4.615  1.00  5.80      COFA C
HETATM   45  C6P PCA   169       7.011 -13.301   5.180  1.00  5.89      COFA C
HETATM   46  O4P PCA   169      10.254 -14.843   4.822  1.00  5.95      COFA O1-
HETATM   47  H2  PCA   169       4.598 -12.001   5.458  1.00  0.00      COFA H
HETATM   48  H3  PCA   169       5.895 -12.224   8.233  1.00  0.00      COFA H
HETATM   49  H2P PCA   169       8.155 -12.965   8.360  1.00  0.00      COFA H
HETATM   50  H3P PCA   169      10.117 -14.119   7.352  1.00  0.00      COFA H
HETATM   51  H5P PCA   169       8.059 -14.273   3.580  1.00  0.00      COFA H
HETATM   52  H6P PCA   169       6.125 -13.133   4.583  1.00  0.00      COFA H
ENDMDL
MODEL        2
ATOM      1  CB  TYR A  42      15.191 -19.501   5.277  1.00  6.58      ACHN C
ATOM      2  CG  TYR A  42      14.455 -18.187   5.400  1.00  5.70      ACHN C
ATOM      3  CD1 TYR A  42      15.140 -16.966   5.441  1.00  6.28      ACHN C
ATOM      4  CD2 TYR A  42      13.063 -18.158   5.570  1.00  5.86      ACHN C
ATOM      5  CE1 TYR A  42      14.484 -15.766   5.704  1.00  6.24      ACHN C
ATOM      6  CE2 TYR A  42      12.382 -16.965   5.804  1.00  5.54      ACHN C
ATOM      7  CZ  TYR A  42      13.100 -15.770   5.901  1.00  5.87      ACHN C
ATOM      8  OH  TYR A  42      12.382 -14.649   6.205  1.00  6.38      ACHN O
ATOM      9 1HB  TYR A  42      16.030 -19.541   5.980  1.00  0.00      ACHN H
ATOM     10 2HB  TYR A  42      14.503 -20.299   5.559  1.00  0.00      ACHN H
ATOM     11  HD1 TYR A  42      16.208 -16.960   5.271  1.00  0.00      ACHN H
ATOM     12  HD2 TYR A  42      12.499 -19.086   5.526  1.00  0.00      ACHN H
ATOM     13  HE1 TYR A  42      15.053 -14.843   5.774  1.00  0.00      ACHN H
ATOM     14  HE2 TYR A  42      11.304 -16.926   5.899  1.00  0.00      ACHN H
ATOM     15  HH  TYR A  42      12.864 -13.823   6.052  1.00  0.00      ACHN H
ATOM     16  CB  GLU A  46      14.133 -14.895   1.909  1.00  5.29      ACHN C
ATOM     17  CG  GLU A  46      12.731 -14.876   2.548  1.00  5.41      ACHN C
ATOM     18  CD  GLU A  46      11.624 -14.157   1.777  1.00  5.62      ACHN C
ATOM     19  OE1 GLU A  46      11.831 -13.543   0.731  1.00  7.37      ACHN O
ATOM     20  OE2 GLU A  46      10.415 -14.196   2.298  1.00  6.10      ACHN O
ATOM     21 1HB  GLU A  46      14.806 -15.492   2.530  1.00  0.00      ACHN H
ATOM     22 2HB  GLU A  46      14.079 -15.392   0.939  1.00  0.00      ACHN H
ATOM     23 1HG  GLU A  46      12.735 -14.451   3.557  1.00  0.00      ACHN H
ATOM     24 2HG  GLU A  46      12.413 -15.908   2.715  1.00  0.00      ACHN H
ATOM     25  HE2 GLU A  46      10.332 -14.593   3.291  1.00  0.00      ACHN H
ATOM     26  CB  THR A  50      11.579 -10.973   5.447  1.00  6.77      ACHN C
ATOM     27  OG1 THR A  50      12.704 -11.842   5.735  1.00  6.60      ACHN O
ATOM     28  CG2 THR A  50      10.828 -11.392   4.187  1.00  7.11      ACHN C
ATOM     29  HB  THR A  50      10.893 -11.108   6.287  1.00  0.00      ACHN H
ATOM     30  HG1 THR A  50      13.243 -11.909   4.921  1.00  0.00      ACHN H
ATOM     31 1HG2 THR A  50      11.433 -11.342   3.277  1.00  0.00      ACHN H
ATOM     32 2HG2 THR A  50       9.940 -10.768   4.048  1.00  0.00      ACHN H
ATOM     33 3HG2 THR A  50      10.500 -12.422   4.297  1.00  0.00      ACHN H
ATOM     34  SG  CYS A  69       2.132 -11.228   6.347  1.00  6.37      ACHN S
TER      35      CYS A  69
HETATM   36  C1  PCA   169       3.535 -11.795   7.344  1.00  6.48      COFA C
HETATM   37  O1  PCA   169       3.462 -12.054   8.544  1.00  7.12      COFA O
HETATM   38  C2  PCA   169       4.730 -11.965   6.558  1.00  6.31      COFA C
HETATM   39  C3  PCA   169       5.912 -12.323   7.151  1.00  6.56      COFA C
HETATM   40  C1P PCA   169       7.048 -12.891   6.503  1.00  5.76      COFA C
HETATM   41  C2P PCA   169       8.219 -13.238   7.222  1.00  6.08      COFA C
HETATM   42  C3P PCA   169       9.277 -13.900   6.630  1.00  6.45      COFA C
HETATM   43  C4P PCA   169       9.223 -14.269   5.243  1.00  5.49      COFA C
HETATM   44  C5P PCA   169       8.021 -13.948   4.537  1.00  5.80      COFA C
HETATM   45  C6P PCA   169       6.983 -13.298   5.147  1.00  5.89      COFA C
HETATM   46  O4P PCA   169      10.188 -14.876   4.648  1.00  5.95      COFA O1-
HETATM   47  H2  PCA   169       4.622 -11.954   5.483  1.00  0.00      COFA H
```

```
HETATM   48  H3  PCA   169       5.956 -12.248   8.237  1.00  0.00      COFA H
HETATM   49  H2P PCA   169       8.254 -13.002   8.284  1.00  0.00      COFA H
HETATM   50  H3P PCA   169      10.166 -14.178   7.186  1.00  0.00      COFA H
HETATM   51  H5P PCA   169       7.950 -14.273   3.504  1.00  0.00      COFA H
HETATM   52  H6P PCA   169       6.072 -13.127   4.589  1.00  0.00      COFA H
ENDMDL
MODEL        3
ATOM      1  CB  PHE A  42      24.203  -3.384 -17.498  1.00  8.99      ACHN C
ATOM      2  CG  PHE A  42      22.704  -3.528 -17.641  1.00  8.71      ACHN C
ATOM      3  CD1 PHE A  42      22.092  -4.784 -17.743  1.00  9.89      ACHN C
ATOM      4  CD2 PHE A  42      21.903  -2.382 -17.763  1.00 10.09      ACHN C
ATOM      5  CE1 PHE A  42      20.528  -2.493 -17.971  1.00 11.22      ACHN C
ATOM      6  CE2 PHE A  42      20.726  -4.902 -17.982  1.00 11.92      ACHN C
ATOM      7  CZ  PHE A  42      19.941  -3.754 -18.089  1.00 11.89      ACHN C
ATOM      8 1HB  PHE A  42      24.717  -4.045 -18.205  1.00  0.00      ACHN H
ATOM      9 2HB  PHE A  42      24.473  -2.361 -17.764  1.00  0.00      ACHN H
ATOM     10  HD1 PHE A  42      22.695  -5.676 -17.627  1.00  0.00      ACHN H
ATOM     11  HD2 PHE A  42      22.363  -1.399 -17.703  1.00  0.00      ACHN H
ATOM     12  HE1 PHE A  42      19.903  -1.607 -18.027  1.00  0.00      ACHN H
ATOM     13  HE2 PHE A  42      20.283  -5.889 -18.068  1.00  0.00      ACHN H
ATOM     14  HZ  PHE A  42      18.867  -3.817 -18.202  1.00  0.00      ACHN H
ATOM     15  CB  GLU A  46      19.851  -4.871 -14.120  1.00  7.73      ACHN C
ATOM     16  CG  GLU A  46      19.106  -3.745 -14.853  1.00  7.73      ACHN C
ATOM     17  CD  GLU A  46      17.974  -3.112 -14.063  1.00  8.06      ACHN C
ATOM     18  OE1 GLU A  46      17.771  -3.369 -12.886  1.00 10.86      ACHN O
ATOM     19  OE2 GLU A  46      17.191  -2.257 -14.705  1.00  9.41      ACHN O
ATOM     20 1HB  GLU A  46      20.707  -5.191 -14.719  1.00  0.00      ACHN H
ATOM     21 2HB  GLU A  46      20.244  -4.489 -13.177  1.00  0.00      ACHN H
ATOM     22 1HG  GLU A  46      18.711  -4.055 -15.822  1.00  0.00      ACHN H
ATOM     23 2HG  GLU A  46      19.820  -2.960 -15.109  1.00  0.00      ACHN H
ATOM     24  HE2 GLU A  46      17.369  -2.256 -15.727  1.00  0.00      ACHN H
ATOM     25  CB  THR A  50      14.683  -4.407 -17.413  1.00  8.56      ACHN C
ATOM     26  OG1 THR A  50      16.053  -4.634 -17.735  1.00  8.92      ACHN O
ATOM     27  CG2 THR A  50      14.473  -3.644 -16.101  1.00 10.24      ACHN C
ATOM     28  HB  THR A  50      14.217  -3.799 -18.211  1.00  0.00      ACHN H
ATOM     29  HG1 THR A  50      16.583  -3.834 -17.508  1.00  0.00      ACHN H
ATOM     30 1HG2 THR A  50      15.076  -4.057 -15.287  1.00  0.00      ACHN H
ATOM     31 2HG2 THR A  50      13.416  -3.670 -15.811  1.00  0.00      ACHN H
ATOM     32 3HG2 THR A  50      14.760  -2.599 -16.217  1.00  0.00      ACHN H
ATOM     33  SG  CYS A  69      10.744   3.716 -18.418  1.00  8.13      ACHN S
TER      34      CYS A  69
HETATM   35  C1  PCA   169      11.886   2.788 -19.454  1.00  8.11      COFA C
HETATM   36  O1  PCA   169      12.004   2.963 -20.663  1.00  8.50      COFA O
HETATM   37  C2  PCA   169      12.687   1.844 -18.712  1.00  8.26      COFA C
HETATM   38  C3  PCA   169      13.510   0.986 -19.377  1.00  9.14      COFA C
HETATM   39  C1P PCA   169      14.563   0.203 -18.815  1.00  8.12      COFA C
HETATM   40  C2P PCA   169      15.295  -0.685 -19.632  1.00  9.31      COFA C
HETATM   41  C3P PCA   169      16.298  -1.473 -19.107  1.00  9.03      COFA C
HETATM   42  C4P PCA   169      16.611  -1.431 -17.720  1.00  8.71      COFA C
HETATM   43  C5P PCA   169      15.966  -0.433 -16.931  1.00  8.24      COFA C
HETATM   44  C6P PCA   169      14.968   0.344 -17.468  1.00  8.31      COFA C
HETATM   45  O4P PCA   169      17.422  -2.302 -17.196  1.00  9.42      COFA O1-
HETATM   46  H2  PCA   169      12.711   1.929 -17.638  1.00  0.00      COFA H
HETATM   47  H3  PCA   169      13.396   0.935 -20.459  1.00  0.00      COFA H
HETATM   48  H2P PCA   169      15.065  -0.723 -20.694  1.00  0.00      COFA H
HETATM   49  H3P PCA   169      16.868  -2.163 -19.716  1.00  0.00      COFA H
HETATM   50  H5P PCA   169      16.250  -0.328 -15.891  1.00  0.00      COFA H
HETATM   51  H6P PCA   169      14.485   1.083 -16.842  1.00  0.00      COFA H
ENDMDL
MODEL        4
ATOM      1  CB  TYR A  42      15.319 -19.629   5.318  1.00 10.33      ACHN C
ATOM      2  CG  TYR A  42      14.621 -18.293   5.452  1.00  9.08      ACHN C
ATOM      3  CD1 TYR A  42      15.327 -17.085   5.546  1.00 10.50      ACHN C
```

```
ATOM      4  CD2 TYR A  42      13.226 -18.236   5.560  1.00  9.44      ACHN C
ATOM      5  CE1 TYR A  42      14.682 -15.866   5.745  1.00 10.98      ACHN C
ATOM      6  CE2 TYR A  42      12.558 -17.025   5.740  1.00  9.70      ACHN C
ATOM      7  CZ  TYR A  42      13.287 -15.832   5.827  1.00 10.01      ACHN C
ATOM      8  OH  TYR A  42      12.646 -14.630   5.963  1.00 11.26      ACHN O
ATOM      9 1HB  TYR A  42      16.163 -19.696   6.013  1.00  0.00      ACHN H
ATOM     10 2HB  TYR A  42      14.609 -20.407   5.601  1.00  0.00      ACHN H
ATOM     11  HD1 TYR A  42      16.406 -17.097   5.443  1.00  0.00      ACHN H
ATOM     12  HD2 TYR A  42      12.647 -19.153   5.509  1.00  0.00      ACHN H
ATOM     13  HE1 TYR A  42      15.250 -14.945   5.816  1.00  0.00      ACHN H
ATOM     14  HE2 TYR A  42      11.475 -16.996   5.795  1.00  0.00      ACHN H
ATOM     15  HH  TYR A  42      11.698 -14.740   5.608  1.00  0.00      ACHN H
ATOM     16  C   ALA A  45      16.733 -12.602   0.482  1.00 10.31      ACHN C
ATOM     17  O   ALA A  45      16.212 -11.463   0.604  1.00 11.94      ACHN O
ATOM     18  N   GLU A  46      16.134 -13.727   0.941  1.00  9.34      ACHN N
ATOM     19  CA  GLU A  46      14.893 -13.645   1.687  1.00  9.44      ACHN C
ATOM     20  C   GLU A  46      15.072 -12.893   3.002  1.00  9.65      ACHN C
ATOM     21  O   GLU A  46      14.170 -12.120   3.360  1.00 11.07      ACHN O
ATOM     22  CB  GLU A  46      14.271 -15.028   1.930  1.00  9.25      ACHN C
ATOM     23  CG  GLU A  46      12.908 -14.942   2.615  1.00  9.03      ACHN C
ATOM     24  CD  GLU A  46      11.832 -14.235   1.809  1.00  9.88      ACHN C
ATOM     25  OE1 GLU A  46      12.032 -13.731   0.714  1.00 13.31      ACHN O
ATOM     26  OE2 GLU A  46      10.620 -14.173   2.361  1.00 10.58      ACHN O
ATOM     27  HN  GLU A  46      16.602 -14.627   0.845  1.00  0.00      ACHN H
ATOM     28  HA  GLU A  46      14.192 -13.034   1.119  1.00  0.00      ACHN H
ATOM     29 1HB  GLU A  46      14.940 -15.638   2.545  1.00  0.00      ACHN H
ATOM     30 2HB  GLU A  46      14.166 -15.540   0.970  1.00  0.00      ACHN H
ATOM     31 1HG  GLU A  46      12.988 -14.422   3.573  1.00  0.00      ACHN H
ATOM     32 2HG  GLU A  46      12.559 -15.947   2.865  1.00  0.00      ACHN H
ATOM     33  HE2 GLU A  46      10.580 -14.531   3.313  1.00  0.00      ACHN H
ATOM     34  N   GLY A  47      16.214 -13.119   3.701  1.00 10.10      ACHN N
ATOM     35  HN  GLY A  47      16.956 -13.713   3.346  1.00  0.00      ACHN H
ATOM     36  C   ILE A  49      13.007  -8.439   3.474  1.00 12.34      ACHN C
ATOM     37  O   ILE A  49      12.340  -7.423   3.689  1.00 16.54      ACHN O
ATOM     38  N   THR A  50      13.125  -9.461   4.358  1.00 10.55      ACHN N
ATOM     39  CA  THR A  50      12.209  -9.554   5.476  1.00 10.97      ACHN C
ATOM     40  C   THR A  50      12.793  -9.186   6.837  1.00 10.87      ACHN C
ATOM     41  O   THR A  50      12.026  -9.028   7.805  1.00 12.74      ACHN O
ATOM     42  CB  THR A  50      11.632 -10.979   5.571  1.00 11.86      ACHN C
ATOM     43  OG1 THR A  50      12.715 -11.788   6.023  1.00 12.02      ACHN O
ATOM     44  CG2 THR A  50      11.011 -11.427   4.255  1.00 14.25      ACHN C
ATOM     45  HN  THR A  50      13.641 -10.299   4.080  1.00  0.00      ACHN H
ATOM     46  HA  THR A  50      11.402  -8.840   5.300  1.00  0.00      ACHN H
ATOM     47  HB  THR A  50      10.842 -10.957   6.335  1.00  0.00      ACHN H
ATOM     48  HG1 THR A  50      12.677 -12.715   5.728  1.00  0.00      ACHN H
ATOM     49 1HG2 THR A  50      11.753 -11.503   3.461  1.00  0.00      ACHN H
ATOM     50 2HG2 THR A  50      10.232 -10.717   3.956  1.00  0.00      ACHN H
ATOM     51 3HG2 THR A  50      10.537 -12.398   4.371  1.00  0.00      ACHN H
ATOM     52  N   GLY A  51      14.130  -9.088   6.923  1.00 11.03      ACHN N
ATOM     53  HN  GLY A  51      14.759  -9.316   6.149  1.00  0.00      ACHN H
ATOM     54  C   PRO A  68       0.297 -14.380   9.570  1.00  9.11      ACHN C
ATOM     55  O   PRO A  68      -0.862 -14.722   9.353  1.00  9.91      ACHN O
ATOM     56  N   CYS A  69       0.847 -13.281   8.979  1.00  9.11      ACHN N
ATOM     57  CA  CYS A  69       0.114 -12.583   7.950  1.00  8.97      ACHN C
ATOM     58  C   CYS A  69      -0.200 -13.438   6.714  1.00  9.19      ACHN C
ATOM     59  O   CYS A  69      -1.042 -12.984   5.938  1.00 11.39      ACHN O
ATOM     60  CB  CYS A  69       0.792 -11.264   7.537  1.00 10.53      ACHN C
ATOM     61  SG  CYS A  69       2.149 -11.403   6.312  1.00 10.26      ACHN S
ATOM     62  HN  CYS A  69       1.826 -13.046   9.118  1.00  0.00      ACHN H
ATOM     63  HA  CYS A  69      -0.876 -12.325   8.342  1.00  0.00      ACHN H
ATOM     64 1HB  CYS A  69       1.172 -10.724   8.404  1.00  0.00      ACHN H
ATOM     65 2HB  CYS A  69       0.076 -10.606   7.045  1.00  0.00      ACHN H
ATOM     66  N   THR A  70       0.494 -14.600   6.539  1.00  8.79      ACHN N
```

```
ATOM     67  HN  THR A  70       1.127 -14.952   7.254  1.00  0.00      ACHN H
TER      68      THR A  70
HETATM   69  C1  PCA   126       3.519 -11.964   7.312  1.00  9.67      COFA C
HETATM   70  O1  PCA   126       3.397 -12.198   8.520  1.00 10.80      COFA O
HETATM   71  C2  PCA   126       4.746 -12.162   6.571  1.00  9.61      COFA C
HETATM   72  C3  PCA   126       5.912 -12.488   7.197  1.00  9.76      COFA C
HETATM   73  C1P PCA   126       7.091 -13.030   6.584  1.00  9.21      COFA C
HETATM   74  C2P PCA   126       8.238 -13.321   7.355  1.00 10.62      COFA C
HETATM   75  C3P PCA   126       9.348 -13.934   6.802  1.00 10.75      COFA C
HETATM   76  C4P PCA   126       9.363 -14.300   5.425  1.00  9.39      COFA C
HETATM   77  C5P PCA   126       8.192 -14.041   4.662  1.00  9.61      COFA C
HETATM   78  C6P PCA   126       7.100 -13.429   5.227  1.00  9.49      COFA C
HETATM   79  O4P PCA   126      10.404 -14.849   4.858  1.00 11.14      COFA O1-
HETATM   80  H2  PCA   126       4.670 -12.167   5.491  1.00  0.00      COFA H
HETATM   81  H3  PCA   126       5.928 -12.407   8.283  1.00  0.00      COFA H
HETATM   82  H2P PCA   126       8.228 -13.078   8.414  1.00  0.00      COFA H
HETATM   83  H3P PCA   126      10.222 -14.158   7.407  1.00  0.00      COFA H
HETATM   84  H5P PCA   126       8.186 -14.348   3.622  1.00  0.00      COFA H
HETATM   85  H6P PCA   126       6.217 -13.275   4.621  1.00  0.00      COFA H
ENDMDL
MODEL        5
ATOM      1  CB  TYR A  42      15.260 -19.581   5.240  1.00 10.05      ACHN C
ATOM      2  CG  TYR A  42      14.569 -18.245   5.381  1.00 10.58      ACHN C
ATOM      3  CD1 TYR A  42      15.281 -17.048   5.526  1.00 11.49      ACHN C
ATOM      4  CD2 TYR A  42      13.173 -18.195   5.517  1.00 10.50      ACHN C
ATOM      5  CE1 TYR A  42      14.638 -15.852   5.851  1.00  8.34      ACHN C
ATOM      6  CE2 TYR A  42      12.510 -17.010   5.815  1.00  9.92      ACHN C
ATOM      7  CZ  TYR A  42      13.249 -15.840   6.006  1.00  8.85      ACHN C
ATOM      8  OH  TYR A  42      12.540 -14.732   6.370  1.00 14.96      ACHN O
ATOM      9 1HB  TYR A  42      16.121 -19.639   5.915  1.00  0.00      ACHN H
ATOM     10 2HB  TYR A  42      14.559 -20.357   5.556  1.00  0.00      ACHN H
ATOM     11  HD1 TYR A  42      16.359 -17.056   5.406  1.00  0.00      ACHN H
ATOM     12  HD2 TYR A  42      12.600 -19.112   5.434  1.00  0.00      ACHN H
ATOM     13  HE1 TYR A  42      15.220 -14.951   6.017  1.00  0.00      ACHN H
ATOM     14  HE2 TYR A  42      11.432 -16.957   5.899  1.00  0.00      ACHN H
ATOM     15  HH  TYR A  42      13.017 -13.894   6.262  1.00  0.00      ACHN H
ATOM     16  C   ALA A  45      16.650 -12.566   0.502  1.00 10.39      ACHN C
ATOM     17  O   ALA A  45      16.112 -11.465   0.655  1.00 13.81      ACHN O
ATOM     18  N   GLU A  46      16.037 -13.706   0.936  1.00 10.16      ACHN N
ATOM     19  CA  GLU A  46      14.783 -13.637   1.683  1.00 11.15      ACHN C
ATOM     20  C   GLU A  46      14.970 -12.958   3.034  1.00 10.71      ACHN C
ATOM     21  O   GLU A  46      14.055 -12.232   3.493  1.00 11.19      ACHN O
ATOM     22  CB  GLU A  46      14.148 -15.030   1.900  1.00 11.13      ACHN C
ATOM     23  CG  GLU A  46      12.782 -14.990   2.598  1.00  7.80      ACHN C
ATOM     24  CD  GLU A  46      11.706 -14.248   1.816  1.00 10.18      ACHN C
ATOM     25  OE1 GLU A  46      11.960 -13.703   0.746  1.00 17.11      ACHN O
ATOM     26  OE2 GLU A  46      10.493 -14.203   2.329  1.00 13.93      ACHN O
ATOM     27  HN  GLU A  46      16.493 -14.611   0.816  1.00  0.00      ACHN H
ATOM     28  HA  GLU A  46      14.080 -13.011   1.137  1.00  0.00      ACHN H
ATOM     29 1HB  GLU A  46      14.825 -15.661   2.484  1.00  0.00      ACHN H
ATOM     30 2HB  GLU A  46      14.032 -15.507   0.924  1.00  0.00      ACHN H
ATOM     31 1HG  GLU A  46      12.843 -14.543   3.593  1.00  0.00      ACHN H
ATOM     32 2HG  GLU A  46      12.442 -16.011   2.786  1.00  0.00      ACHN H
ATOM     33  HE2 GLU A  46      10.357 -14.648   3.278  1.00  0.00      ACHN H
ATOM     34  N   GLY A  47      16.137 -13.189   3.659  1.00  6.92      ACHN N
ATOM     35  HN  GLY A  47      16.847 -13.792   3.247  1.00  0.00      ACHN H
ATOM     36  C   ILE A  49      12.843  -8.477   3.748  1.00 14.28      ACHN C
ATOM     37  O   ILE A  49      12.183  -7.464   3.962  1.00 20.93      ACHN O
ATOM     38  N   THR A  50      12.983  -9.513   4.596  1.00 11.91      ACHN N
ATOM     39  CA  THR A  50      12.085  -9.692   5.710  1.00 11.47      ACHN C
ATOM     40  C   THR A  50      12.653  -9.186   7.033  1.00 13.16      ACHN C
ATOM     41  O   THR A  50      11.901  -8.918   7.980  1.00 10.61      ACHN O
ATOM     42  CB  THR A  50      11.709 -11.192   5.769  1.00 10.53      ACHN C
```

```
ATOM     43  OG1 THR A  50      12.908 -11.956   5.963  1.00 16.50      ACHN O
ATOM     44  CG2 THR A  50      10.910 -11.628   4.550  1.00  9.91      ACHN C
ATOM     45  HN  THR A  50      13.528 -10.300   4.254  1.00  0.00      ACHN H
ATOM     46  HA  THR A  50      11.184  -9.097   5.533  1.00  0.00      ACHN H
ATOM     47  HB  THR A  50      11.077 -11.348   6.641  1.00  0.00      ACHN H
ATOM     48  HG1 THR A  50      13.361 -12.100   5.097  1.00  0.00      ACHN H
ATOM     49 1HG2 THR A  50      11.423 -11.412   3.615  1.00  0.00      ACHN H
ATOM     50 2HG2 THR A  50       9.936 -11.131   4.550  1.00  0.00      ACHN H
ATOM     51 3HG2 THR A  50      10.739 -12.700   4.594  1.00  0.00      ACHN H
ATOM     52  N   GLY A  51      13.994  -9.104   7.107  1.00 12.26      ACHN N
ATOM     53  HN  GLY A  51      14.585  -9.352   6.316  1.00  0.00      ACHN H
ATOM     54  C   PRO A  68       0.470 -14.478   9.346  1.00  8.81      ACHN C
ATOM     55  O   PRO A  68      -0.704 -14.795   9.156  1.00 10.22      ACHN O
ATOM     56  N   CYS A  69       1.053 -13.403   8.710  1.00 10.41      ACHN N
ATOM     57  CA  CYS A  69       0.406 -12.694   7.628  1.00 12.79      ACHN C
ATOM     58  C   CYS A  69      -0.200 -13.648   6.600  1.00 11.30      ACHN C
ATOM     59  O   CYS A  69      -1.238 -13.320   6.041  1.00 15.51      ACHN O
ATOM     60  CB  CYS A  69       1.365 -11.803   6.775  1.00 12.83      ACHN C
ATOM     61  SG  CYS A  69       2.772 -11.079   7.644  1.00 15.87      ACHN S
ATOM     62  HN  CYS A  69       2.005 -13.154   8.949  1.00  0.00      ACHN H
ATOM     63  HA  CYS A  69      -0.422 -12.089   8.004  1.00  0.00      ACHN H
ATOM     64 1HB  CYS A  69       0.786 -10.980   6.350  1.00  0.00      ACHN H
ATOM     65 2HB  CYS A  69       1.820 -12.389   5.970  1.00  0.00      ACHN H
ATOM     66  N   THR A  70       0.571 -14.744   6.321  1.00  9.30      ACHN N
ATOM     67  HN  THR A  70       1.357 -14.962   6.927  1.00  0.00      ACHN H
TER      68      THR A  70
HETATM   69  C1  PCA   169       4.213 -11.814   6.779  1.00  9.26      COFA C
HETATM   70  O1  PCA   169       4.084 -12.570   5.825  1.00 13.20      COFA O
HETATM   71  C2  PCA   169       5.414 -11.352   7.438  1.00  5.57      COFA C
HETATM   72  C3  PCA   169       6.685 -11.869   7.513  1.00  6.49      COFA C
HETATM   73  C1P PCA   169       7.418 -12.861   6.805  1.00 12.80      COFA C
HETATM   74  C2P PCA   169       8.650 -13.290   7.372  1.00 10.20      COFA C
HETATM   75  C3P PCA   169       9.522 -14.115   6.703  1.00 12.07      COFA C
HETATM   76  C4P PCA   169       9.249 -14.504   5.347  1.00  9.86      COFA C
HETATM   77  C5P PCA   169       7.957 -14.172   4.830  1.00 11.85      COFA C
HETATM   78  C6P PCA   169       7.073 -13.380   5.528  1.00  9.66      COFA C
HETATM   79  O4P PCA   169      10.149 -15.081   4.628  1.00 20.99      COFA O1-
HETATM   80  H2  PCA   169       5.240 -10.522   8.107  1.00  0.00      COFA H
HETATM   81  H3  PCA   169       7.276 -11.396   8.301  1.00  0.00      COFA H
HETATM   82  H2P PCA   169       8.889 -12.948   8.377  1.00  0.00      COFA H
HETATM   83  H3P PCA   169      10.470 -14.421   7.128  1.00  0.00      COFA H
HETATM   84  H5P PCA   169       7.715 -14.522   3.832  1.00  0.00      COFA H
HETATM   85  H6P PCA   169       6.116 -13.115   5.096  1.00  0.00      COFA H
ENDMDL
MODEL        6
ATOM      1  CB  TYR A  42      15.288 -19.590   5.256  1.00 10.05      ACHN C
ATOM      2  CG  TYR A  42      14.572 -18.268   5.397  1.00 10.58      ACHN C
ATOM      3  CD1 TYR A  42      15.253 -17.047   5.513  1.00 11.49      ACHN C
ATOM      4  CD2 TYR A  42      13.178 -18.250   5.525  1.00 10.50      ACHN C
ATOM      5  CE1 TYR A  42      14.572 -15.849   5.736  1.00  8.34      ACHN C
ATOM      6  CE2 TYR A  42      12.480 -17.065   5.740  1.00  9.92      ACHN C
ATOM      7  CZ  TYR A  42      13.178 -15.854   5.827  1.00  8.85      ACHN C
ATOM      8  OH  TYR A  42      12.492 -14.674   5.968  1.00 14.96      ACHN O
ATOM      9 1HB  TYR A  42      16.164 -19.628   5.912  1.00  0.00      ACHN H
ATOM     10 2HB  TYR A  42      14.609 -20.378   5.591  1.00  0.00      ACHN H
ATOM     11  HD1 TYR A  42      16.333 -17.031   5.414  1.00  0.00      ACHN H
ATOM     12  HD2 TYR A  42      12.630 -19.186   5.496  1.00  0.00      ACHN H
ATOM     13  HE1 TYR A  42      15.114 -14.915   5.819  1.00  0.00      ACHN H
ATOM     14  HE2 TYR A  42      11.400 -17.066   5.829  1.00  0.00      ACHN H
ATOM     15  HH  TYR A  42      11.566 -14.828   5.573  1.00  0.00      ACHN H
ATOM     16  C   ALA A  45      16.650 -12.566   0.502  1.00 10.39      ACHN C
ATOM     17  O   ALA A  45      16.112 -11.465   0.655  1.00 13.81      ACHN O
ATOM     18  N   GLU A  46      16.039 -13.708   0.923  1.00 10.16      ACHN N
```

```
ATOM     19  CA  GLU A  46      14.788 -13.641   1.672  1.00 11.15      ACHN C
ATOM     20  C   GLU A  46      14.968 -12.943   3.021  1.00 10.71      ACHN C
ATOM     21  O   GLU A  46      14.067 -12.202   3.450  1.00 11.19      ACHN O
ATOM     22  CB  GLU A  46      14.154 -15.030   1.879  1.00 11.13      ACHN C
ATOM     23  CG  GLU A  46      12.810 -14.969   2.610  1.00  7.80      ACHN C
ATOM     24  CD  GLU A  46      11.717 -14.239   1.853  1.00 10.18      ACHN C
ATOM     25  OE1 GLU A  46      11.905 -13.722   0.762  1.00 17.11      ACHN O
ATOM     26  OE2 GLU A  46      10.517 -14.164   2.428  1.00 13.93      ACHN O
ATOM     27  HN  GLU A  46      16.508 -14.608   0.816  1.00  0.00      ACHN H
ATOM     28  HA  GLU A  46      14.091 -13.009   1.123  1.00  0.00      ACHN H
ATOM     29 1HB  GLU A  46      14.834 -15.667   2.452  1.00  0.00      ACHN H
ATOM     30 2HB  GLU A  46      14.015 -15.504   0.906  1.00  0.00      ACHN H
ATOM     31 1HG  GLU A  46      12.917 -14.481   3.582  1.00  0.00      ACHN H
ATOM     32 2HG  GLU A  46      12.467 -15.982   2.836  1.00  0.00      ACHN H
ATOM     33  HE2 GLU A  46      10.448 -14.586   3.348  1.00  0.00      ACHN H
ATOM     34  N   GLY A  47      16.137 -13.189   3.659  1.00  6.92      ACHN N
ATOM     35  HN  GLY A  47      16.846 -13.794   3.253  1.00  0.00      ACHN H
ATOM     36  C   ILE A  49      12.843  -8.477   3.748  1.00 14.28      ACHN C
ATOM     37  O   ILE A  49      12.183  -7.464   3.962  1.00 20.93      ACHN O
ATOM     38  N   THR A  50      12.943  -9.514   4.612  1.00 11.91      ACHN N
ATOM     39  CA  THR A  50      12.035  -9.582   5.734  1.00 11.47      ACHN C
ATOM     40  C   THR A  50      12.651  -9.120   7.049  1.00 13.16      ACHN C
ATOM     41  O   THR A  50      11.920  -8.814   8.007  1.00 10.61      ACHN O
ATOM     42  CB  THR A  50      11.477 -11.009   5.872  1.00 10.53      ACHN C
ATOM     43  OG1 THR A  50      12.575 -11.809   6.298  1.00 16.50      ACHN O
ATOM     44  CG2 THR A  50      10.828 -11.477   4.577  1.00  9.91      ACHN C
ATOM     45  HN  THR A  50      13.446 -10.357   4.324  1.00  0.00      ACHN H
ATOM     46  HA  THR A  50      11.211  -8.891   5.544  1.00  0.00      ACHN H
ATOM     47  HB  THR A  50      10.704 -10.974   6.653  1.00  0.00      ACHN H
ATOM     48  HG1 THR A  50      12.545 -12.737   5.993  1.00  0.00      ACHN H
ATOM     49 1HG2 THR A  50      11.564 -11.620   3.785  1.00  0.00      ACHN H
ATOM     50 2HG2 THR A  50      10.087 -10.738   4.255  1.00  0.00      ACHN H
ATOM     51 3HG2 THR A  50      10.303 -12.416   4.732  1.00  0.00      ACHN H
ATOM     52  N   GLY A  51      13.994  -9.104   7.107  1.00 12.26      ACHN N
ATOM     53  HN  GLY A  51      14.572  -9.388   6.318  1.00  0.00      ACHN H
ATOM     54  C   PRO A  68       0.470 -14.478   9.346  1.00  8.81      ACHN C
ATOM     55  O   PRO A  68      -0.704 -14.795   9.156  1.00 10.22      ACHN O
ATOM     56  N   CYS A  69       1.051 -13.404   8.707  1.00 10.41      ACHN N
ATOM     57  CA  CYS A  69       0.392 -12.699   7.629  1.00 12.79      ACHN C
ATOM     58  C   CYS A  69      -0.209 -13.658   6.604  1.00 11.30      ACHN C
ATOM     59  O   CYS A  69      -1.249 -13.337   6.046  1.00 15.51      ACHN O
ATOM     60  CB  CYS A  69       1.335 -11.802   6.766  1.00 12.83      ACHN C
ATOM     61  SG  CYS A  69       2.739 -11.060   7.623  1.00 15.87      ACHN S
ATOM     62  HN  CYS A  69       2.001 -13.149   8.946  1.00  0.00      ACHN H
ATOM     63  HA  CYS A  69      -0.439 -12.102   8.011  1.00  0.00      ACHN H
ATOM     64 1HB  CYS A  69       0.746 -10.986   6.344  1.00  0.00      ACHN H
ATOM     65 2HB  CYS A  69       1.788 -12.386   5.959  1.00  0.00      ACHN H
ATOM     66  N   THR A  70       0.571 -14.744   6.321  1.00  9.30      ACHN N
ATOM     67  HN  THR A  70       1.354 -14.963   6.930  1.00  0.00      ACHN H
TER      68      THR A  70
HETATM   69  C1  PCA   169       4.175 -11.803   6.781  1.00  9.26      COFA C
HETATM   70  O1  PCA   169       4.073 -12.578   5.842  1.00 13.20      COFA O
HETATM   71  C2  PCA   169       5.370 -11.312   7.442  1.00  5.57      COFA C
HETATM   72  C3  PCA   169       6.634 -11.814   7.558  1.00  6.49      COFA C
HETATM   73  C1P PCA   169       7.388 -12.829   6.891  1.00 12.80      COFA C
HETATM   74  C2P PCA   169       8.579 -13.257   7.525  1.00 10.20      COFA C
HETATM   75  C3P PCA   169       9.485 -14.080   6.896  1.00 12.07      COFA C
HETATM   76  C4P PCA   169       9.275 -14.464   5.538  1.00  9.86      COFA C
HETATM   77  C5P PCA   169       8.024 -14.136   4.946  1.00 11.85      COFA C
HETATM   78  C6P PCA   169       7.106 -13.340   5.600  1.00  9.66      COFA C
HETATM   79  O4P PCA   169      10.228 -15.042   4.856  1.00 20.99      COFA O1-
HETATM   80  H2  PCA   169       5.180 -10.463   8.080  1.00  0.00      COFA H
HETATM   81  H3  PCA   169       7.212 -11.310   8.335  1.00  0.00      COFA H
```

```
HETATM   82  H2P PCA   169       8.768 -12.919   8.539  1.00  0.00      COFA H
HETATM   83  H3P PCA   169      10.402 -14.384   7.389  1.00  0.00      COFA H
HETATM   84  H5P PCA   169       7.838 -14.474   3.932  1.00  0.00      COFA H
HETATM   85  H6P PCA   169       6.177 -13.065   5.114  1.00  0.00      COFA H
ENDMDL
END
```